ESTIMATION OF SALT-SOLUTIONED CAVERN SIZE AND SHAPE FROM SURFACE TROUGH WIDTH AND DEPTH UNDER SUPER-CRITICAL CONDITION USING PHYSICAL MODEL

Naruemol Saoanunt

A Thesis Submitted in Partial Fulfillment of the Requirements for the Doctor of Philosophy of Engineering in Civil Transportation and Geo-resource

Suranaree University of Technology

Academic Year 2018

การประเมินขนาดและรูปร่างโพรงเกลือจากความกว้างและความลึกของร่องการทรุดตัวภายใต้สภาวะเกินกว่าจุดวิกฤติโดยใช้แบบจำลองเชิงกายภาพ

นางสาวนฤมล เสาอนันต์

วิทยานิพนธ์นี้เป็นส่วนหนึ่งของการศึกษาตามหลักสูตรปริญญาวิศวกรรมศาสตรดุษฎีบัณฑิต
สาขาวิชาวิศวกรรมโยธา ขนส่ง และทรัพยากรธรณี
มหาวิทยาลัยเทคโนโลยีสุรนารี
ปีการศึกษา 2561

ESTIMATION OF SALT-SOLUTIONED CAVERN SIZE AND SHAPE FROM SURFACE TROUGH WIDTH AND DEPTH UNDER SUPER-CRITICAL CONDITION USING PHYSICAL MODEL

Suranaree University of Technology has approved this thesis submitted in partial fulfillment of the requirements for the Degree of Doctor of Philosophy

Thesis Examining Committee

(Assoc. Prof. Dr. Pornkasem Jongpradist)
Chairperson

(Prof. Dr. Kittitep Fuenkajorn)
Member (Thesis Advisor)

(Asst. Prof. Dr. Akkhapun Wannakomol)
Member

(Asst. Prof. Dr. Decho Phueakphum)
Member

(Asst. Prof. Dr. Prachya Tepnarong)
Member

(Prof. Dr. Santi Maensiri)
Vice Rector for Academic Affairs and Internationalization

(Assoc. Prof. Flt. Lt. Dr. Kontorn Chamniprasart)
Dean of Institute of Engineering

นฤมล เสาอนันต์ : การประเมินขนาดและรูปร่างโพรงเกลือจากความกว้างและความลึกของร่องการทรุดตัวภายใต้สภาวะเกินกว่าจุดวิกฤติโดยใช้แบบจำลองเชิงกายภาพ (ESTIMATION OF SALT-SOLUTIONED CAVERN SIZE AND SHAPE FROM SURFACE TROUGH WIDTH AND DEPTH UNDER SUPER-CRITICAL CONDITION USING PHYSICAL MODEL) อาจารย์ที่ปรึกษา : ศาสตราจารย์ ดร.กิตติเทพ เฟื่องขจร, 93 หน้า.

แบบจำลองทางกายภาพได้ดำเนินการโดยใช้โครงจำลองทางกายภาพ (trap door apparatus) เพื่อจำลองการทรุดตัวของผิวดินที่มีผลกระทบของขนาดและรูปร่างของโพรงเกลือที่เกิดจากการละลายบริเวณรอยต่อระหว่างชั้นเกลือหินและชั้นดินปิดทับด้านบน ทรายละเอียด (2 มิลลิเมตร) ได้นำมาเพื่อจำลองชั้นหินปิดทับ การทรุดตัวสูงสุดและความกว้างของการทรุดตัวถูกวัดด้วยเลเซอร์สแกนเนอร์ใน 3 มิติ การจำลองโดยใช้ระเบียบวิธีการเชิงตัวเลขด้วยโปรแกรม PFC เพื่อนำมาเปรียบเทียบกับผลการจำลองทางกายภาพ และสร้างความสัมพันธ์กับรูปร่างของโพรงเกลือภายใต้ความเค้นยึดติดและมุมเสียดทานของชั้นหินปิดทับในระดับต่างกัน ผลการทดสอบระบุว่าความลึกและความกว้างของการทรุดตัวของผิวดินมีค่าเพิ่มขึ้นเมื่อโพรงละลายเกลือมีความกว้างและความสูงมากขึ้น ภายใต้ความสูงของโพรงที่เท่ากัน การทรุดตัวสูงสุดมีค่าลดลงเพียงเล็กน้อยเมื่อชั้นหินปิดทับมีความหนามากขึ้น ผลการจำลองทางคอมพิวเตอร์มีความสอดคล้องกับผลที่ได้จากแบบจำลองทางกายภาพเป็นอย่างดี ชุดของสมการเชิงประจักษ์ถูกพัฒนาขึ้นเพื่ออธิบายผลการทดสอบและผลที่ได้จากแบบจำลองด้วยคอมพิวเตอร์ ซึ่งสมการดังกล่าวสามารถนำมาประเมินความสูงและความกว้างของโพรงเกลือโดยใช้ข้อมูลจากรูปทรงของการทรุดตัวบนผิวดินและคุณสมบัติเชิงกลศาสตร์ของชั้นหินปิดทับ

สาขาวิชา เทคโนโลยีธรณี ลายมือชื่อนักศึกษา นฤมล เสาอนันต์

ปีการศึกษา 2561 ลายมือชื่ออาจารย์ที่ปรึกษา

NARUEMOL SAOANUNT : ESTIMATION OF SALT-SOLUTIONED CAVERN SIZE AND SHAPE FROM SURFACE TROUGH WIDTH AND DEPTH UNDER SUPER-CRITICAL CONDITION USING PHYSICAL MODEL. THESIS ADVISOR : PROF. KITTITEP FUENKAJORN, Ph.D., 93 PP.

SUBSIDENCE/CAVERN/SALT/PHYSICAL MODEL

Physical model tests are performed using a trap door apparatus to simulate surface subsidence as affected by size and shape of salt-solution caverns created at the interface between salt and overlying soil formations. Fine sand (2 mm) is used as overburden material. The maximum subsidence and trough width are measured using 3-D laser scanner. Numerical simulations using PFC code are performed to compare with the model results and to correlate the cavern geometries under a variety of cohesions and friction angles of the overburden. The results indicate that the surface subsidence and trough width increase with increasing cavern width and height. Under the same cavern height, the maximum subsidence slightly decreases with increasing the overburden thickness. The computer model results agree well with those obtained from the physical model results. Set of empirical equations is derived to fit with the physical model results, which can be used to estimate the cavern height and width from the subsidence trough configurations and overburden mechanical properties.

School of Geotechnology

Academic Year 2018

Student's Signature นฤมล เสาอนันต์

Advisor's Signature

ACKNOWLEDGMENTS

The author wishes to acknowledge the support from the Suranaree University of Technology who has provided funding for this research.

Grateful thanks and appreciation are given to Prof. Dr. Kittitep Fuenkajorn for his valuable guidance and gave a critical review of this study. I appreciate his strong support, encouragement, suggestions, and comments during the research period. Many thanks to Assoc. Prof. Dr. Pornkasem Jongpradist, Asst. Prof. Dr. Decho Phueakphum, Asst. Prof. Dr. Prachya Tepnarong, and Asst. Prof. Dr. Akkhapun Wannakomol for their constructive advice, valuable suggestions, and comments on my study. Grateful thanks are given to all staffs of Geomechanics Research Unit, Institute of Engineering who supported my work.

Finally, I would like to thank my parents for their support and encouragement.

Naruemol Saoanunt

TABLE OF CONTENTS

Page

TABLE OF CONTENTS (Continued)

Page

TABLE OF CONTENTS (Continued)

Page

LIST OF TABLES

Table **Page**

LIST OF FIGURES

Figure **Page**

LIST OF FIGURES (Continued)

Figure **Page**

LIST OF FIGURES (Continued)

Figure **Page**

LIST OF FIGURES (Continued)

Figure **Page**

LIST OF FIGURES (Continued)

Figure **Page**

SYMBOLS AND ABBREVIATIONS

α	=	Empirical constant
β	=	Empirical constant
γ	=	Angle of draw
A	=	Empirical constant
B	=	Empirical constant
B	=	Width of trough
B_e	=	Equivalent trough width
B_s	=	Block size (or particle size)
C	=	Empirical constant
D	=	Empirical constant
C_c	=	Coefficient of curvature
C_u	=	Uniformity coefficient
c	=	Cohesion
H	=	Opening height
H_e	=	Equivalent opening height
K_n	=	Normal stiffness
K_s	=	Joint shear stiffness
L	=	Opening length
S_e	=	Equivalent maximum subsidence
S_{max}	=	Maximum magnitude of subsidence
W	=	Opening width

SYMBOLS AND ABBREVIATIONS (Continued)

W_e	=	Equivalent opening width
Z	=	Overburden thickness
Z_e	=	Equivalent opening depth (or Equivalent overburden thickness)
ϕ	=	Friction angle

CHAPTER I

INTRODUCTION

1.1 Background and rationale

Salt and associated minerals in the Khorat and Sakon Nakhon basins, northeast of Thailand have become important resources for mineral exploitation and for use as host rock for product storage. For over five decades, local people have extracted the salt near ground surface by using an old-fashioned technique, called here the 'brine pumping' method. A shallow borehole is drilled into the rock unit directly above the salt. Brine (saline groundwater) is pumped through the borehole and left to evaporate on the ground surface. This simple and low-cost method can, however, cause an environmental impact in the form of unpredictable ground subsidence, sinkholes, and surface contamination (Fuenkajorn, 2002). The subsidence or sinkhole is caused by deformation or collapse of the cavern roof at the interface between the salt and overburden. This usually occurs during dry season where the cavities loss the support from the groundwater. Exploratory drilling and geophysical methods (e.g., resistivity and seismic surveys) have normally been employed to determine the size, depth, and location of the underground cavities in the problem areas in an attempt to backfill the underground voids, and hence minimize the damage to the engineering structures and farmland on the surface (Wannakao et al., 2005; Jenkunawat, 2005; and Jenkunawat, 2007). The geophysical and drilling investigations for such a widespread area are costly and time-consuming. This calls for a quick and low-cost method to determine the size,

and shape of the solution caverns. The method may be used as an early warning tool so that mitigation can be implemented before the uncontrollable and severe subsiding of the ground surface occurs.

Numerical methods have also been widely employed for the subsidence analysis, primarily to predict the maximum subsidence, and size and shape of the subsidence trough. The extent of subsidence area is predominantly controlled by geological conditions of the overburden strata. A variety of numerical codes have been used ranging from non-linear, linearly elastic, plastic, to visco-elastic plastic models (Liu et al., 2011; Fuenkajorn and Archeeploha, 2011; Helm et al., 2013; Li et al., 2011; and Lisjak and Grasselli, 2004). The main drawback of the numerical approaches is that they require representative material parameters and accurate boundary and loading conditions of the simulated domains. This means that extensive laboratory and field testing and measurements are required to obtain the representative input parameters.

Physical modelling has long been a research tool for understanding of the subsidence mechanisms (Terzaghi, 1936; Adachi et al., 2003, and Ghabraie et al., 2015). Several modeling techniques has been developed worldwide to study the ground responses to the underground excavations. These techniques range from two-dimensional trap door tests to miniature tunnel boring machines that can simulate the process of tunnel excavation and lining installation in a centrifuge (Park., 2004 and Meguid, 2008). The primary advantage of the physical or scaled-down model test is that the boundaries and material properties can be well controlled, and hence provides the results that are isolated from the effects of material inhomogeneity and the complex shape of the underground caverns.

This study is focused on the estimation of the solutioned cavern height and

width at the interface between salt bed and overlying soil formation. Series of physical model simulations and numerical analyses are performed under a variety of cavern sizes, shapes, and depths. Mathematical relationships are proposed to link the cavern geometries with the subsidence trough configurations and overburden properties.

1.2 Research objectives

The objectives of this study are to estimate opening width and height of solution cavern in rock salt by three-dimensional scaled-down simulations platform under super-critical condition, and to determine the mathematical relationship among the subsidence parameters. The results obtained from the physical model are compared with those of the computer model simulations using Particle Flow Code in two Dimensions (PFC^{2D}code) software to assess the accuracy of the test results.

1.3 Scope and limitations

The scope and limitations of the research include as follows.

a) Scaled-down platform or a trap door apparatus (Thongprapha et al., 2015) is used to simulate the surface subsidence under super-critical condition.

b) Granular material (Clean and uniform sand) with nominal size 2 mm is used to simulate the overburden.

c) The cavern configurations are varied as follows; width = 10 to 50 mm, length = 200 mm, and height = 25 to 100 mm.

d) Each series of test is simulated at least 3 times to verify the repeatability of the results.

e) The overburden thickness is varied from 100 mm to 300 mm.

f) Maximum subsidence depth and width of trough is determined.

g) All tests are made under ambient temperature.

h) Physical model results are correlated with numerical simulations (using PFC^{2D} code).

1.4 Research methodology

Figure 1.1 shows the research methodology, including literature review, material simulating overburden, physical models, computer simulations are using Particle Flow in 2-dimension Code (PFC^{2D}), correlation between physical and numerical simulations, formulation of mathematical relationship, discussions, and conclusions.

1.4.1 Literature review

Literature review will be carried out to enhance an understanding of surface subsidence knowledge and the subsidence prediction methods. The sources of information are from journals, technical reports, and conference papers. A summary of the literature review will be given in the thesis.

1.4.2 Material simulating overburden

Granular material with nominal size 2 mm is used as the overburden test material. The material is subjected to 2 tests; grain size analysis and direct shear test. The grain size analysis is performed to determine the percentage of different grain sizes contained within a material. The objective of direct shear test is to determine the cohesion and the friction angle.

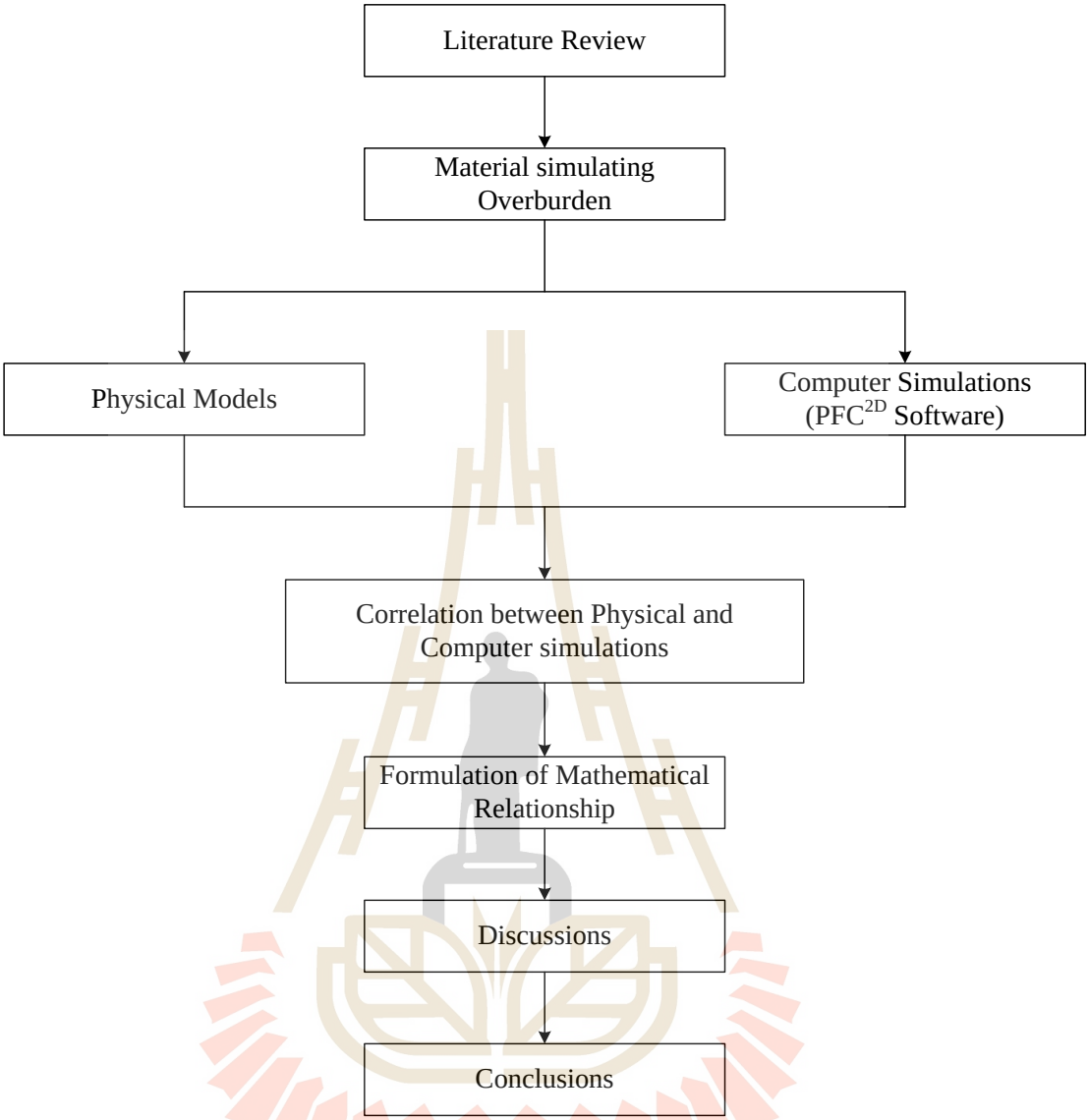

Figure 1.1 Research methodology.

1.4.3 Physical models

A test frame for physical model as developed by Thongprapha et al. (2015) is used to simulate subsidence of overburden in three-dimension. The laboratory testing gives the maximum surface subsidence (S_{max}) and the width of subsidence trough. The model testing is simulated for the opening width (W) from 10 mm to 50 mm with and increment of 20 mm. The opening length (L) is 250 mm all cases. The

opening height (H) is from 25 mm to 100 mm, with 25 mm increment. In this study, overburden thickness (Z) is varied from 100 mm to 300 mm. A laser scanner is used to measures the surface profile of the granular material before and after the subsidence is induced.

1.4.4 Computer simulations

The computer code is used to correlate and calculate the subsidence characteristics of the test model by considering the effects of underground caverns. The calculation is carried out with PFC^{2D} software (Itasca, 2008) which is based on Distinct Element Method and it is performed in following 5 steps:

1. Determination of material behavior model and material properties.
2. Formation of the model geometry.
3. Determination of the boundaries and initial condition; initial running of the program and monitoring of the model response.
4. Re-evaluation of the model and necessary modifications.
5. Interpretation of the result.

1.4.5 Correlation between physical and computer simulations

Results obtained from physical model in laboratory tests is used to correlate with the computer simulations result from the Particles Flow in 2 dimensions code. The material properties of computer simulations are same with the physical model.

1.4.6 Formulation of mathematical relationships

The results from the simulations are used to develop mathematic relationships between the maximum surface subsidence (S_{max}) and width of trough (B)

and overburden thickness (Z). Such relationships are later used to predict cavern configuration (cavern size; opening width, opening height and depth).

1.4.7 Discussions and conclusions

Discussions are on the reliability and adequacies of the approaches used here. Future research needs are identified. All research activities, methods, and results are documented and complied in the thesis. The findings are published in the journals or conference proceedings.

1.4.8 Thesis writing and presentation

Thesis writing and presentation All research activities, methods, and results are documented and compiled in the thesis.

1.5 Thesis contents

This research thesis is divided into six chapters. The first chapter includes background and rationale, research objectives, scope and limitations and research methodology. The second chapter presents results of the literature review to improve an understanding of surface subsidence knowledge. The Chapter three describes materials simulating overburden and physical model simulations. Computer Simulations by PFC^{2D} software and comparison between the results obtained from physical model computer simulation are described in chapter four. Formulation and mathematical relationships are describing in chapter five. Chapter six presents discussions, conclusions, and recommendation for future studies.

CHAPTER II

LITERATURE REVIEW

2.1 Introduction

Relevant topics and previous research results are reviewed to improve an understanding of surface subsidence. These include the surface subsidence or sinkholes in Thailand, theory and criteria, the estimations of subsidence and Particle Flow Code in 2 Dimensions (PFC^{2D}). The review results are summarized below.

2.2 Subsidence (Sinkholes) in Thailand

The Northeastern Thailand covering area of 160,000 km^2 is in the Khorat Plateau and is composed of two tectonic basins, Khorat and Sakon Nakorn basins (Figure 2.1). The two basins cover areas of 46,000 km^2 (Satarugsa et al., 2005, 2011). Subsurface geology of the two basins consists of unconsolidated sediments overlaying deformed claystone and rock salt layers of Maha Sarakham formation. Figure 2.2 shows a typical stratigraphic section of the Maha Sarakham formation. The basin covers the area of Nakhon Ratchasima, Chaiyaphum, Khon Kaen, Maha Sarakham, Roi Et, Kalasin, Yasothon, Ubon Ratchathani provinces and the north of Burirum, Surin, and Sisaket provinces (Suwanich, 1986). Figure 2.3 also shows the areas where the brine pumping has been practices. Depths of the shallowest salt in those areas vary from 40 m to 200 m. It belongs to the Middle or Lower member, depending on locations. Most of the brine pumping practices are however in the areas where the

topography is flat, groundwater table is near the surface, and the salt depth is less than 50 m in the Sakon Nakhon basin, and about 100 m in the Khorat basin (Jenkunawat, 2005; Wannakao et al., 2005). Based on field investigation, Jenkunawat (2007) states that the surface subsidence normally occurs in the areas where depth of the shallowest salt is less than 50 m. The overburden consists mainly of mudstone siltstone and sandstone of the Middle Clastic, and claystone and mudstone of the Lower Clastic, with fractures typically dipping less than 30 degrees, and rarely at 70 degrees (Crosby, 2007). The members are characterized by abundant halite and anhydrite-filled fractures and bands with typical thickness of 2 cm to 5 cm.

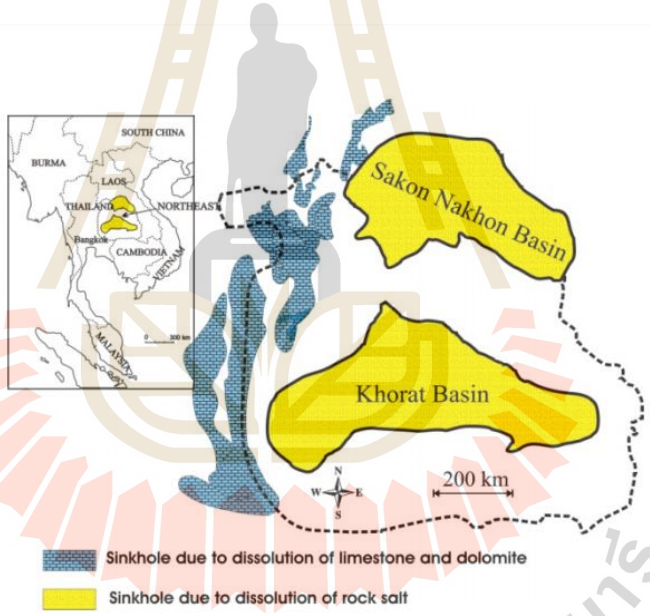

Figure 2.1 Sakon Nakhon and Khorat Basins containing rock salt in the northeast of Thailand (modified from Satarugsa, 2011).

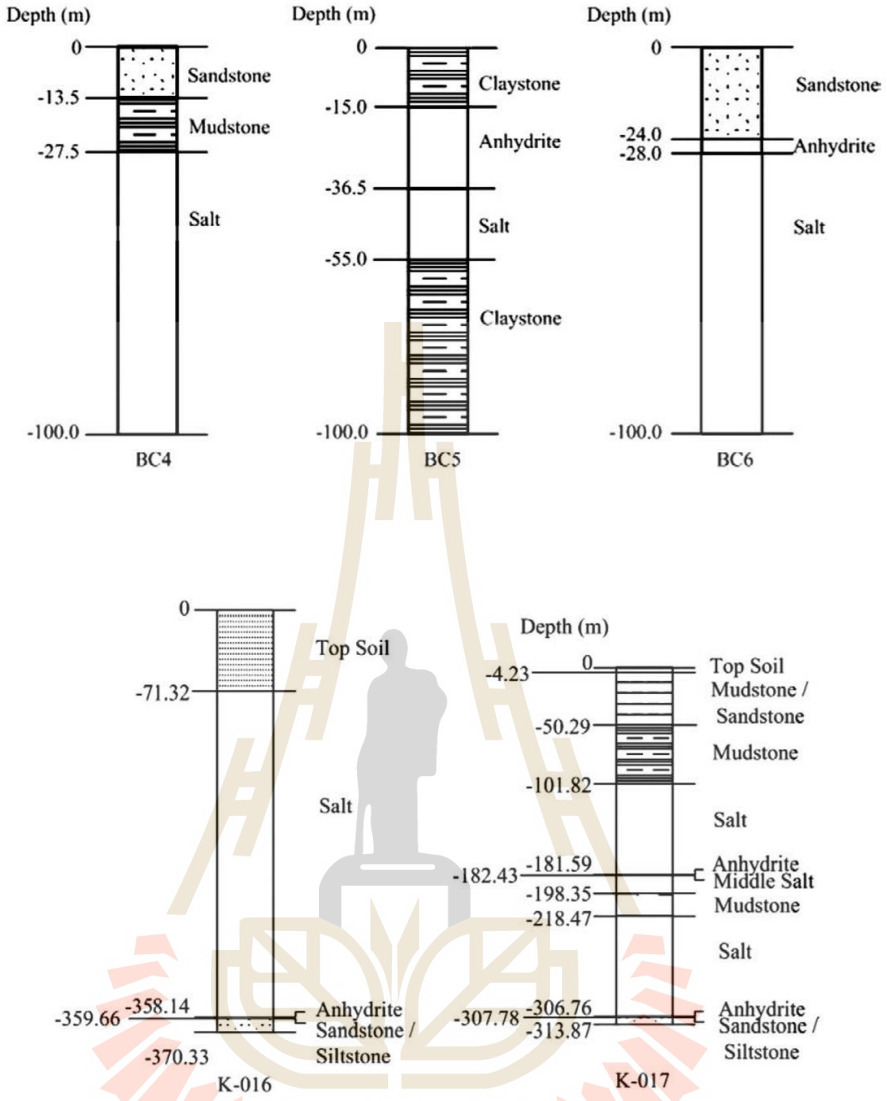

Figure 2.2 Stratigraphic unit from some borehole drilled outside the brine pumping area in Sakon Nakhon basin (top row modified from Jenkunawat, 2005) and in Korat basin (bottom row modified from Vattanasak, 2006).

Figure 2.3 Brine pumping areas in Khorat and Sakon Nakhon salt basins (Fuenkajorn and Archeeploha, 2009).

Wannakao and Walsri (2007) state that one third of the northeast is generally underlain by sedimentary rocks of Maha Sarakham Formation, sequences of rock salt and clastic rocks. The deposits are divided into the Khorat and Sakon Nakhon basins. Salt productions from brine groundwater are common in both basins. A brine groundwater well is 4 in diameter with 2 in air pumping line at about 60-100 meters depth. The brine is pumped to salt storage bin, then conveyed to salt paddy field for solar evaporation. There is many surface subsidence reported in salt production area in Ban Non Sabaeng, Sakon Nakhon province.

Jenkunawat (2007) studies occurrence of salt cavities induced by brine pumping. The main purpose is to delineate disaster area and monitor land subsidence. Drill holes were totally 12 with depth ranged 100-200 m. A number of holes were constructed as 12 monitoring wells to observe circulation patterns of the brine by cased

them with PVC pipes. Drilling results showed claystone at top, salt dome located under the salt production area at depth of 40-50 m. Rock salt was located at depth 40-200 m. Anhydrite and gypsum were observed in holes around the salt dome. Sinkholes are circular in shape, with diameter of 50-100 m. Land usually starts subsiding at pumping well and moves in a series of subsidence which can be traced in a line. They occur in only on a salt dome, where there are fractures, brine zone and dissolution of salt. Areas out of the salt dome are not under risk of salt subsidence.

2.3 Theory and Criteria

Singh (1992) and Hawkes (2010) study the surface subsidence from coal mine and classified characteristics of subsidence by the size of extraction area including subcritical extraction area, critical extraction area and super-critical extraction area as illustrated in figure 2.4 – 2.6, respectively. All three figures present a horizontal coal seam below a horizontal ground surface. Only two dimensions are considered. A portion of the coal seam has been extracted, resulting in a subsidence trough at the surface. For simplicity, the parameters m and h (and consequently the parameters S_{max} and B) are taken as constants in each figure. The subsidence factor, a, is taken to be 1.0 so that the calculated maximum subsidence (S_{max}) is equal to the mined coal thickness (m).

The first schematic (Figure 2.4) represents a subcritical extraction area where the extracted width is less than 2·B.

The second schematic (Figure 2.5) represents a critical extraction area, where the extracted width is equal to 2·B.

The third schematic (Figure 2.6) represents a super-critical extraction area

where the extracted width is greater than 2·B. The maximum amount of subsidence is equal to the calculated value of S_{max} over a finite distance above the center of the extraction area, beginning at a distance B from the edge of the extraction area.

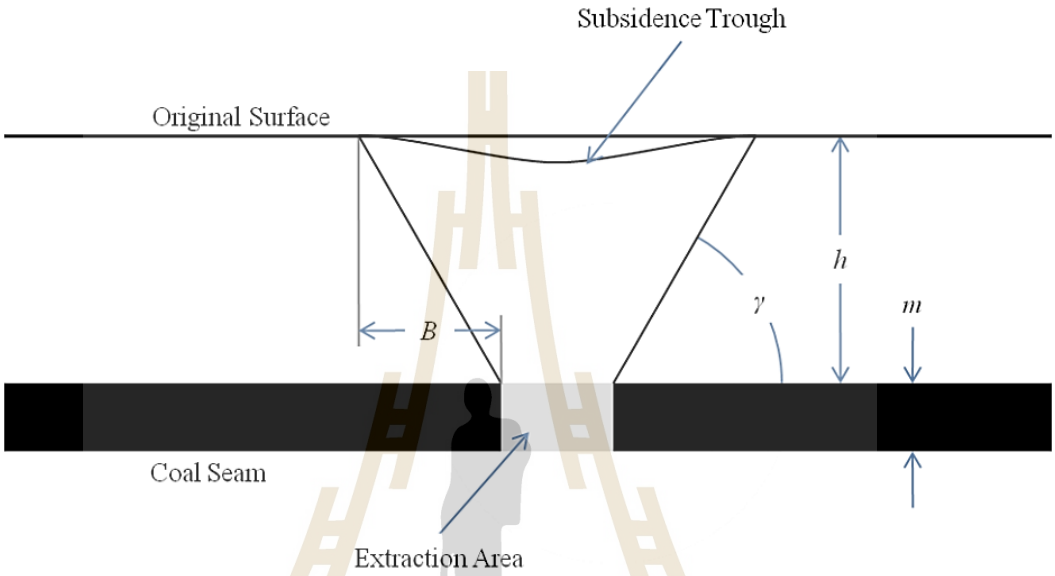

Figure 2.4 Illustration of parameters: subcritical extraction (Hawkes, 2010).

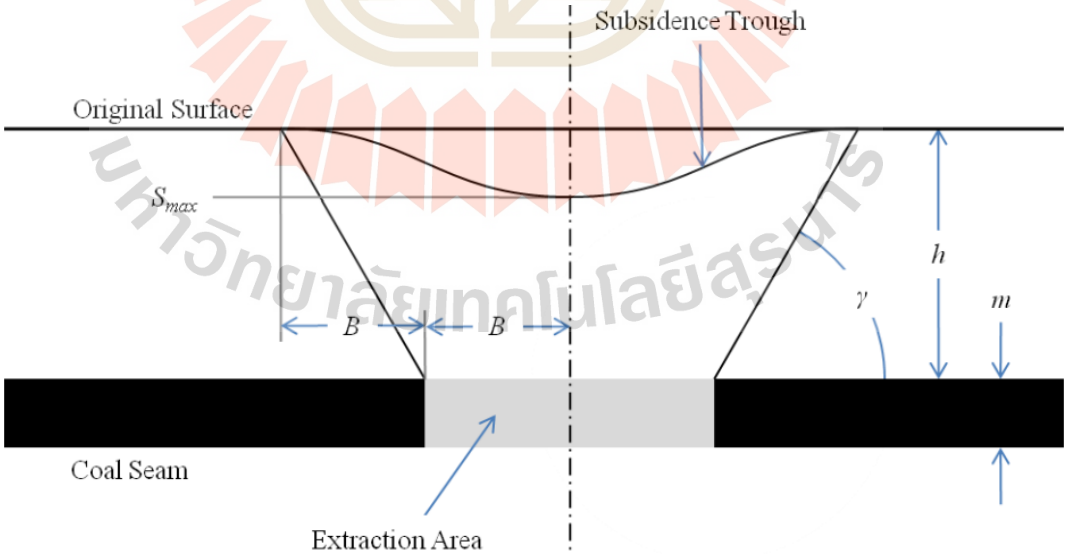

Figure 2.5 Illustration of parameters: critical extraction (Hawkes, 2010).

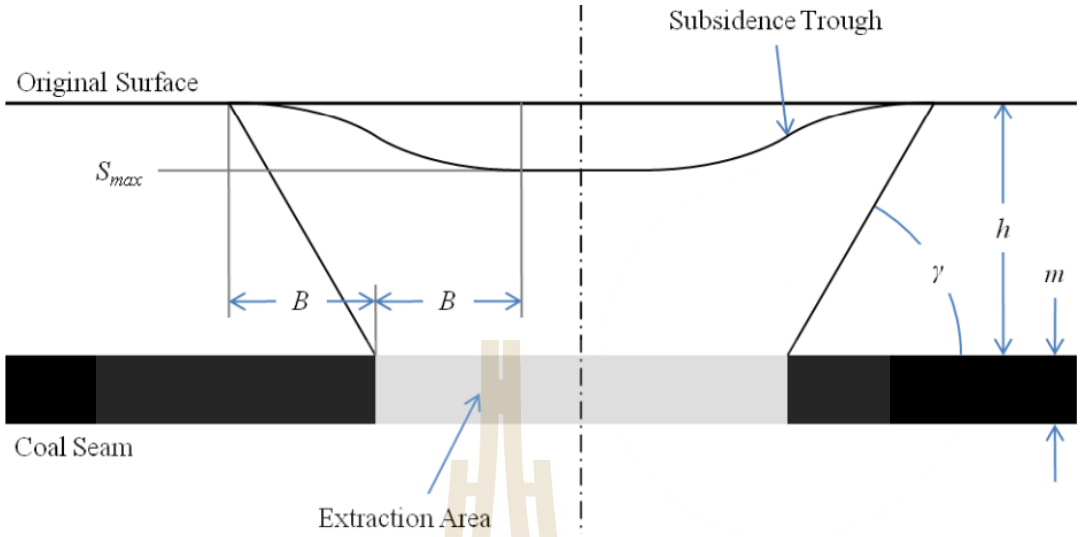

Figure 2.6 Illustration of parameters: supercritical extraction (Hawkes, 2010).

2.4 The estimations of subsidence

There have been numerous methods developed for estimating surface subsidence, such as physical models, empirical approaches, analytical techniques, influence function methods and numerical modelling (Unlu et al., 2013; Alejano et al., 1999; Whittaker and Reddish, 1989; Peng, 1992; Bahuguna et al., 1991).

2.4.1 Physical models

Physical models are helpful for understanding the mechanism of subsidence (Whittaker and Reddish, 1989; Alejano et al., 1999; Asadi et al., 2005). It has been used by many researchers to simulate surface subsidence and other related problems. The advantage of physical modelling is that it allows deformation to occur by natural mechanisms which can be compared to field observations and numerical models. Processes such as caving, surface movements, crack propagation and underground movements can be difficult to produce in numerical models without

incorporating numerous assumptions on strength envelopes to other physical properties. These processes can be investigated by physical modelling (Ghabraie et al., 2014).

One recent study has performed using a trap door apparatus (Figure 2.7) for study the surface subsidence above an underground opening to determine the effect of underground opening or caving configuration on surface subsidence under super-critical condition (Thongprapha et al., 2015). This apparatus has been fabricated to perform the scaled-down simulations of surface subsidence by using gravel and sand to represent the overburden in order to exhibit a cohesionless frictional behavior. They indicate that the importance of the main factors that control the extent of subsidence phenomenon on the surface and determines the effects of geometry of underground openings on the angle of draw, the maximum subsidence and the volume of the subsidence trough. The findings can be used to evaluate the subsidence profile for caverns in soft ground and fractured rock mass. The results show that the maximum subsidence and the angle of draw are controlled by the width (W), length (L), height (H) and depth (Z) of the underground openings.

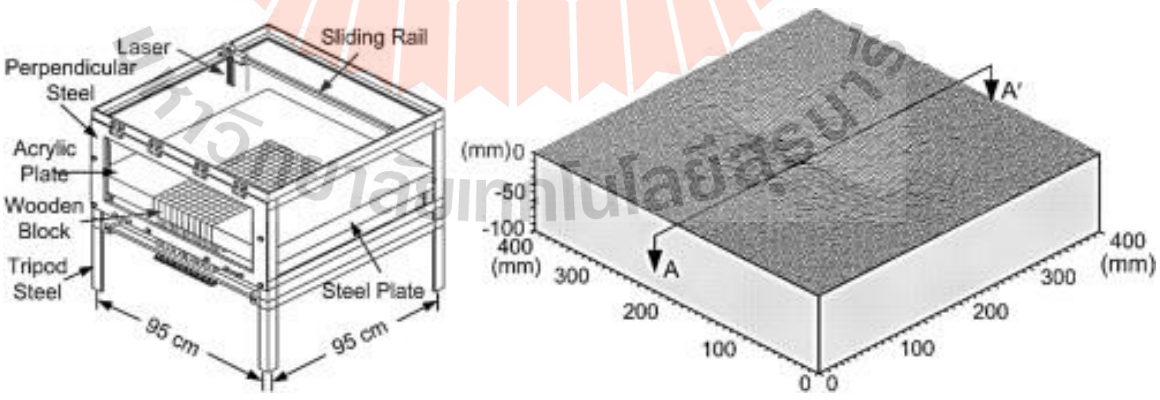

Figure 2.7 Trap door apparatus performed by Thongprapha et al. (2015).

Sartkaew and Fuenkajorn (2016) verify the representativeness and accuracy of the hyperbolic, exponential and trigonometric profile functions by physical model in laboratory tests that have been widely used to define the ground surface subsidence under sub-critical to critical conditions, induced by potash and salt mine openings. Synthetic gel mixed with paraffin additive is used to simulate the overburden for the physical model test. Based on the similarity theory the gel properties, and the opening models can be defined as the prototype that is equivalent to the Maha Sarakham formation. The results obtained from the physical model test agree well with the numerical analyses, suggesting that the laboratory test simulations are reliable and correct (Figure 2.8).

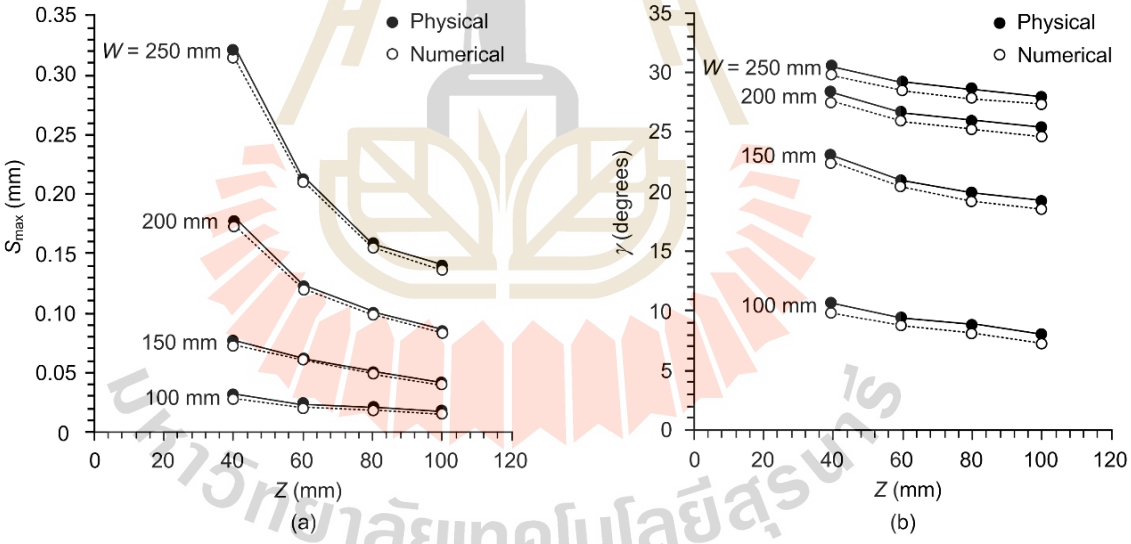

Figure 2.8 Maximum subsidence (a) and (b) angle of draw as a function of opening depth (Sartkaew and Fuenkajorn, 2016).

Saoanunt and Fuenkajorn (2015) study the effects of the mining sequences, excavation rates and overburden slope under super-critical condition by using trap door apparatus. They found that the angle of draw and S_{max}/H ratio decrease with increasing Z/H ratio when the opening height (H) is maintained constant at 50 mm and the opening depth (Z) varies from 50 mm to 200 mm. Consecutive mining sequence from center of panel gives the lowest angle of draw and highest subsidence while excavation from the edge to center of panel causing the highest angle of draw and lowest subsidence. Under various overburden slopes, the angle of draw on up-slope and down-slope increases with increasing slope angle. The S_{max}/H ratio decreases with increasing Z/H ratio and slope angle. The findings can be used to evaluate the subsidence profile for various underground excavation methods as affected by excavation sequence, extraction rate and overburden slope in a heavily fractured rock mass.

Ju et al. (2017) study the effects of sand particle size for simulated coal mining subsidence in physical model tests, uniaxial compressive test was performed. The results indicate that the Young's modulus, uniaxial compressive strength, and tangent modulus were larger in rock-like material samples or overburden materials with finer sand and the failure characteristics changed from mostly shear failure to tensile failure with rising particle sizes. They suggested that the finer sand grain should be used for water-resisting layers (mudstone) while coarser sand grains should be used for aquifer (sandstone) or gas storage rock layers (sandy shale).

Meguid et al. (2008) present the physical models that have developed and used in soft ground tunneling research. Physical modeling of soft ground tunnels is an essential part of the analysis and design of tunnels. Physical models can provide data that can validate and calibrate numerical models. For several decades, numerous researchers

around the world have developed and implemented a variety of techniques to simulate the tunnel excavation process. Reduced scale tests under 1g conditions provide full control over the excavation method. However, they do not accurately simulate the in-situ stress conditions. Centrifuge testing makes a more realistic simulation of in-situ stresses possible, but the tunnel construction process has to be simplified. Different methods have been developed to simulate the process of tunnel construction in soft ground. Soil arching around excavated tunnels has been successfully simulated using the trap door method. Vertical stresses as well as surface displacements can be investigated by lowering a trap door under 2D or 3D conditions. Stability of the tunnel face can be investigated using a rigid tube with flexible membrane at the face. Tunnel excavation is simulated, in this case, by reducing the air pressure inside the tunnel and monitoring the soil movements. Other methods include the dissolvable polystyrene core showed some success; however, the tunneling induced surface settlement is not uniform. In addition, test results were less satisfactory when the excavation is made under water. Techniques based on hand or mechanical augering to represent tunnel excavation and progressive face advance seem more realistic, however, mechanizing the test in the centrifuge is very expensive.

Caudron et al. (2006) study the soil-structure interaction during a sinkhole phenomenon using an analog two-dimensional soil and a physical model and a numerical method. They use bidimensional Schneebeli material (Figure 2.9) in a small-scale model allowing fully controlled test conditions. The Schneebeli material is modified in order to exhibit a cohesive frictional behavior. The physical model allows to represent a case of study and to determine it completely with a limited set of parameters.

Park et al. (2004) state that surface subsidence causes damage such as the failure and deterioration of buildings, infrastructures, dams, underground utility lines, ground water regimes, etc., resulting in severe economic loss and environmental hazards. The major cause of subsidence is underground mining activities. In order to minimize or prevent subsidence damage, it is necessary to understand subsidence phenomena. It is difficult to simulate or predict subsidence development because of the complexity in physical characteristics such as rock failure and yield behavior, dimensional variations and time dependent behavior. In this study, a new physical subsidence modeling technique is introduced. The method utilizes laser optical triangulation distance measurement devices, which can scan the surface of any material, including granular or viscous materials, and digitally measure vertical distances with an extremely high accuracy and resolution. With this new technique, the effect of cavity shape and size, depth, and material parameters can be analyzed. Using this unique technology and method of analysis, significant results were produced. Subsidence profiles, subsidence factors, and angles of draw were analyzed. This research is being continued using the same technique for simulating subsidence with different model materials for various underground cavity dimensions, tunneling, and time dependent subsidence phenomena.

Asadi et al. (2005) propose a new profile function. It is formed from the sum of two negative exponential functions that have been adjusted to three survey lines in a case study in the Negin coalmine east of Iran. Because of the simplicity of the profile function, the use of the new model decreases the calculation time for predicting surface subsidence and enhances the precision of subsidence prediction. The results gained from surface subsidence measurements at Negin coalmine show an excellent

correlation between the measured and the predicted subsidence by using the new model. The correlation coefficient was 0.999, which is very high.

In the empirical method, different graphs and tables are given for different conditions and geometrical shapes. It is possible to predict the amount of subsidence using these graphs and tables. The National Coal Board (NCB) has suggested one of the most well-known graphs for the prediction of subsidence. For example, a graph for the prediction of surface subsidence in horizontal stopes is given in Figure 2.11.

Figure 2.9 Small-scale experimental model (Caudron et al., 2006).

2.4.2 Empirical methods

Empirical method provides the simplest calculation and thus extensively used in practical applications. The most common and widely used empirical method for predicting settlement induced by tunnel is the Peck's formula (Peck, 1969) (Equation 2.1). This classical empirical method is useful for preliminary estimation and initial idea about surface settlement. The formula is as follows:

$$S_v(y) = S_{v\,max} \cdot e^{\frac{-y^2}{2i^2}} \tag{2.1}$$

where S_v (y) is the surface settlement.

$S_{v\,max}$ is the maximum settlement above tunnel axis.

i is the horizontal distance from the tunnel axis to the point of inflection of the settlement trough.

y is the horizontal distance from the tunnel axis.

Peck (1969) described that shape of subsidence examples for more than 20 cases by use the Gaussian curve, shown in Figure 2.10. The researcher presents equation to find shape of trough using subsidence maximum (S_{max}), distance from middle of opening (x) and width of trough (i).

$$i = k \cdot Z_0 \tag{2.2}$$

Many researches have been conducted involving field investigation and tests regarding estimating i. The estimation of i values by various researchers are shown in Table 2.1. The estimation of maximum settlement can be done by Equation 3 (Mair, 1993).

Where, V_L is ground loss (ratio of ground loss volume/tunnel volume per meter length) and D is the tunnel diameter.

$$S_{max} = \frac{0.313 V_L \cdot D^2}{i} \tag{2.3}$$

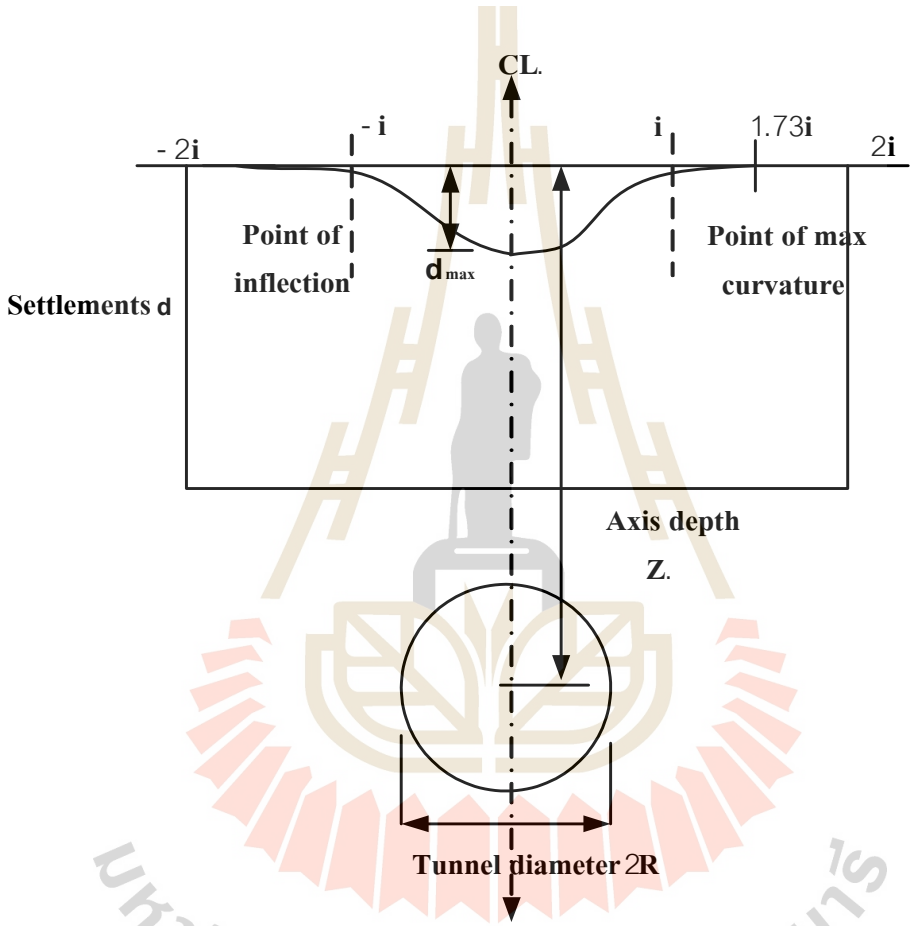

Figure 2.10 Properties of error function curve to represent cross-section settlement trough above tunnel (Peck 1969).

Table 2.1 Recommendations for values of i by various researchers.

Name	Value of *i*	Comment
Peck (1969)	$\frac{i}{R} = \left(\frac{Z_o}{2R}\right)^n$ n = 0.1 to 0.8	Based on field observations
Atkinson and Potts (1977)	$i = 0.25 \cdot (Z_o + R)$ In case of loose sand $i = 0.25 \cdot (1.5Z_o + 0.5R)$ In case of dense sand and over consolidated clay	Base on field observations
O'Reilly and New (1982)	$i = 0.43Z_o + 1.1$ In case of cohesive soil $i = 0.28Z_o - 0.1$ In case of granular soil	Based on field observations of UK tunnels
Mair (1993)	$i = 0.5 \cdot Z_o$	Based on field observations worldwide
Attewell (1977)	$\frac{i}{R} = \alpha \cdot \left(\frac{Z_o}{2R}\right)^n$ α=1 and n=1	Based on field observations of UK tunnels
Clough and Schimdt (1981)	$\frac{i}{R} = \alpha \cdot \left(\frac{Z_o}{2R}\right)^n$ α=1 and n=0.8	Based on field observations USA tunnels

Note: Here, Z_o is the depth of tunnel below ground and R is the tunnel radius.

However, the empirical method which is derived from 20 case histories have no theoretical background and assumes the vertical settlement profile in the ground same as the Gaussian distribution. Moreover, this method is limited by few parameters and unable to address complex situations and other parameters which induce settlement. It also does not cover horizontal displacement and do not consider the impact on any structure interaction. Several authors (Chi et al., 2001; González and Sagaseta, 2001) pointed out some important limitation of this method such as inapplicability to various ground conditions, construction techniques, horizontal movements and subsurface settlements. They are not able to provide solution of tunnel with support. Numerical method provides better solution to overcome these problems. However, the empirical method is useful for comparing the results with the numerical method for validation purpose of a model.

Profile functions are based on a curve fitting procedure that uses a mathematical function to match the measured subsidence profile. When this mathematical function is established by use of actual field data then it can be used for the future prediction of surface subsidence (Peng,1992; Whittaker and Reddish,1989).

Singh (1992) state that the subsidence is an inevitable consequence of underground mining. The empirical methods are consisting graphical, profile functions and influence functions method. The theories of empirical methods are principally based on observations and experience from field subsidence studies. Some of the empirical methods have proved sufficiently reliable for subsidence prediction, at least for a given region.

The major objectives of subsidence engineering are

1. Prediction of ground movement.

2. Determining the effects of such movements on structures and renewable resource.
3. Minimizing damage due to subsidence.

A cavity is created underground, the stress field in the surrounding strata is disturbed. These stress changes produce deformations and displacements of the strata, the extent of which depends on the magnitude of the stresses and the cavity dimensions. With time, supporting structures deteriorate and the cavity enlarges, resulting in instability. This induces the superjacent strata to move into the void. Gradually, these movements work up to the surface, manifesting themselves as a depression. This is commonly referred to as subsidence. Thus, mine subsidence may be defined as ground movements that occur due to the collapse of overlying strata into mine voids. Surface subsidence generally entails both vertical and lateral movements.

Subsidence consists of five major components, which influence damage to surface structures and renewable resources are verticaldisplacement, horizontal displacement, slope, vertical strain, and vertical curvature.

Calculation by empirical method (profile function);

Vertical displacement:

$$S(x) = \frac{1}{2} S_{max} \left[1 - \tanh\left(\frac{cx}{B} \right) \right] \tag{2.4}$$

Slope (or tilt):

$$G(x) = S'(x) = -\frac{1}{2} S_{max} \frac{c}{B} \operatorname{sech}^2\left(\frac{cx}{B} \right) \tag{2.5}$$

Vertical curvature:

$$\rho(x) = S''(x) = S_{max} \frac{c^2}{B^2}\left[\operatorname{sech}^2\left(\frac{cx}{B}\right)\tanh\left(\frac{cx}{B}\right)\right] \quad (2.6)$$

Horizontal displacement (lateral movement):

$$u(x) = -\frac{1}{2} S_{max} \frac{bc}{B}\operatorname{sech}^2\left(\frac{cx}{B}\right) \quad (2.7)$$

Horizontal strain:

$$\varepsilon(x) = S_{max} \frac{bc^2}{B^2}\left[\operatorname{sech}^2\left(\frac{cx}{B}\right)\tanh\left(\frac{cx}{B}\right)\right] \quad (2.8)$$

where S_{max} is the maximum subsidence,

D is depth of cavern,

x is horizontal distance,

c is arbitrary constant,

b is constant, and

B is maximum radius of cavern area.

In the physical method, by combining different materials such as sand and gelatin, a real model, but smaller than the extracted area, has been built. By precise monitoring and processing of data, the amount of subsidence in a real condition is calculated. An example of the physical model is given in Figure 2.12.

In numerical methods, displacements and subsidence of ground surface can be calculated by using finite elements, boundary elements, distinct elements, and finite difference methods. Application of a computer for solving very complex equations in diverse initial and boundary conditions with different material behavior made numerical methods more popular in the prediction of subsidence. In this regard,

different software has been developed to consider inhomogeneous and anisotropic behavior of rock mass worldwide.

2.4.3 Analytical methods

Archeeploha et al. (2009) develop a method to estimate the location, depth and size of caverns created at the interface between salt and overlying formations. A governing hyperbolic equation is used in a statistical analysis of the ground survey data to determine the cavern location, maximum subsidence, maximum surface slope and surface curvature under the sub-critical and critical conditions. A computer program is developed to perform the regression and produce a set of subsidence components and a representative profile of the surface subsidence under sub-critical and critical conditions. Finite difference analyses using FLAC code correlate the subsidence components with the cavern size and depth under a variety of strengths and deformation moduli of the overburden. Set of empirical equations correlates these subsidence components with the cavern configurations and overburden properties. For the super-critical condition, a discrete element method (using UDEC code) is used to demonstrate the uncertainties of the ground movement and sinkhole development resulting from the complexity of the post-failure deformation and joint movements in the overburden. The correlations of the subsidence components with the overburden mechanical properties and cavern geometry are applicable to the range of site conditions specifically imposed here (e.g., half oval -shaped cavern created at the

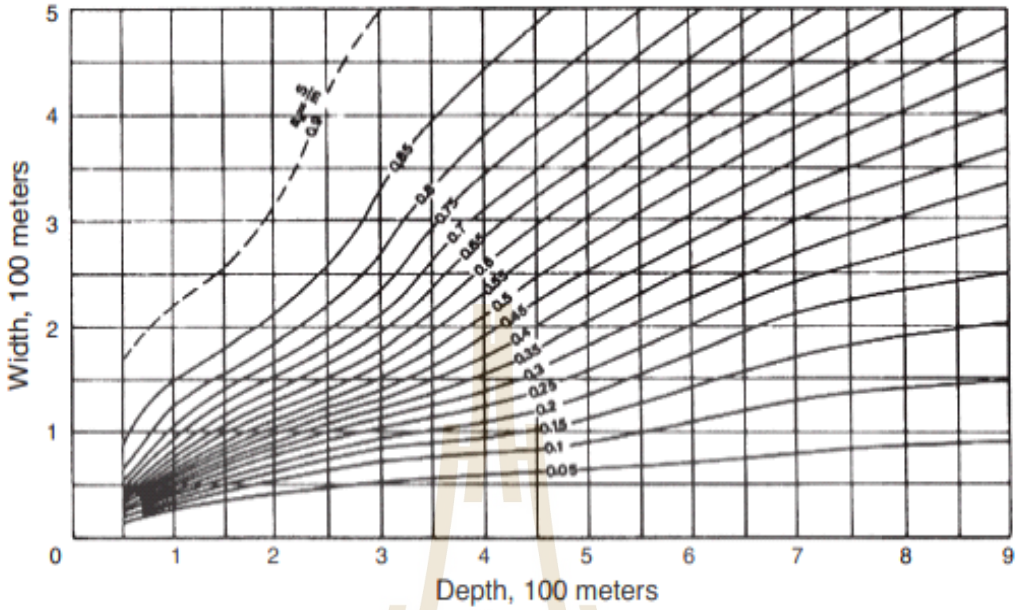

Figure 2.11 Graph suggested by NCE (Asadi et al.,2005).

Figure 2.12 A physical model for prediction of subsidence (Asadi et al., 2005).

overburden-salt interface, horizontal rock units, flat ground surface, and saturated condition). These relations may not be applicable to subsidence induced under different rock characteristics or different configurations of the caverns. The proposed method is not applicable under super-critical conditions where post-failure behavior of the overburden rock mass is not only unpredictable but also complicated by the system of joints, as demonstrated by the results of the discrete element analyses. The proposed method is useful as a predictive tool to identify the configurations of a solution cavern and the corresponding subsidence components induced by the brine pumping practices as shown in Figure 2.13.

Sagaseta (1987) presents a closed-form solution for isotropic and homogeneous incompressible soil due to near-surface ground loss from tunneling. Verruijt and Booker (1996) present a generalization of Sagastea's solution in homogeneous elastic half spaces for the case of ground loss having values of Poisson's ratio which also included the effect of long term tunnel lining deformation or 'ovalization'. However, the analytical solution of Verrujit and Booker was unable to provide a satisfactory agreement with the measured settlement profile. Later Loganathan and Poulos (1998) attempted to refine Verrujit and Booker's solution by incorporating ground loss parameter for tunnels in clay. The refined solution provided better results for tunnels in stiff clay but overestimated for tunnels in soft clay.

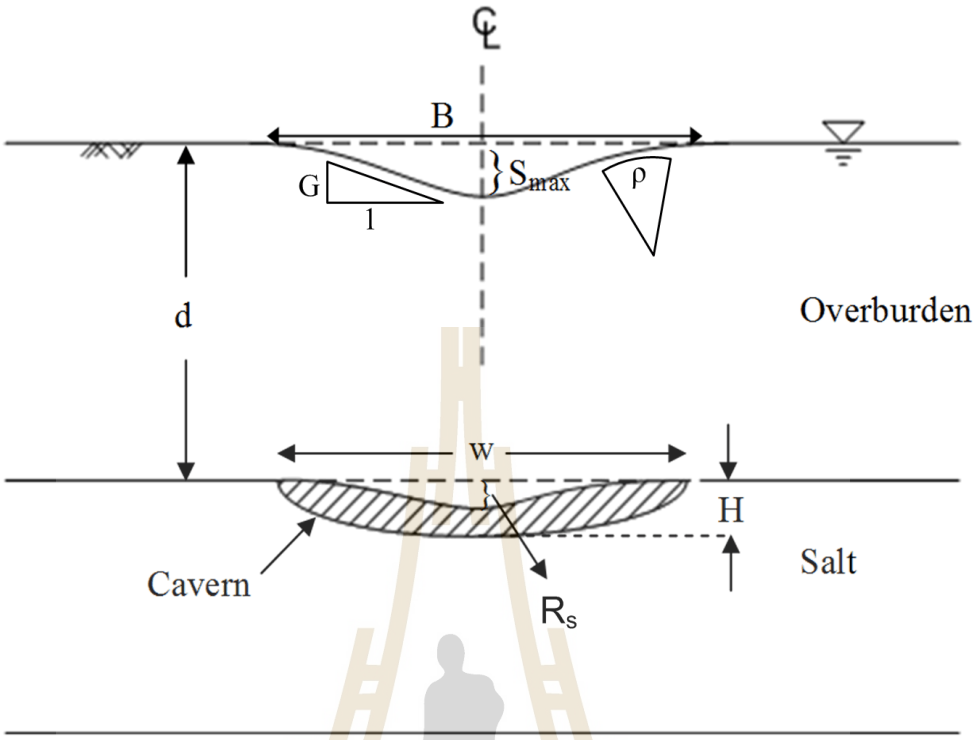

Figure 2.13 Variables using by Archeeploha et al. (2009).

Chi et al. (2001) extend the equivalent ground loss model of Loganathan and Poulos to clayey and sandy soils and the analytical solution was used to conduct back analyses for 29 cases which were performed using optimization principle to obtain key parameters of influence zone angle and gap parameter that provide the best fit to the measured ground settlement profiles.

Bobet (2001) presents an analytical solution for shallow tunnel in saturated ground. Based on method proposed by Bobet (2001), Chou and Bobet (2002) study short term settlement at the ground surface and found good agreement comparing between predictions and actual observations along with correlation between soil and liner, tunnel geometry, and construction procedure. At the tunnel centerline is the gap parameter was mostly responsible for the maximum surface settlements. The limitation

of this analytical solution is that it only gives reasonable predictions for shield driven tunnels in medium to stiff clays, or in soils and soft rocks where plastic deformations around the tunnel are small. And also, because the analytical solution is based on the assumption of elasticity, it tends to predict maximum soil deformations and overestimate the settlement trough. The analytical solution is derived for a specific type of case and problem. Since the ground condition, physical and mechanical properties of soil and rock, also the geometrical properties of tunnel are varying from site to site, it is not applicable to all type of case and cannot deal with complex unique different situation which is a limitation of analytical method.

2.4.4 Numerical methods

The application of numerical methods to real cases has to be accompanied by three processes: calibration of real data, variation and sensitivity analysis (Wang et al., 2003)

Many limitations of empirical methods and analytical methods can be overcome by the numerical method. Apart from geotechnical properties of ground, tunnel geometry and depth the stress-strain condition of both tunnel structure and ground which affect the settlement also rely on the construction process. Numerical method can take into account this construction process called 'step-by-step' method (Galli et al., 2004). The numerical method which constitutes continuum and discontinuum modelling are useful tool for predicting tunnel induced ground settlement. Continnum model includes Finite Element Method (FEM) and FDM (Finite Difference Method) and Discontinnm model include Distinct Element Method (DEM).

Li and Zhu (2007) indicate that various factors of affecting ground settlement can be comprehensively considered by the numerical method, which could

forecast ground settlement caused by the tunnel excavation accurately. Numerical methods can deal with various soil and rock properties, geometrical properties, complex boundary condition and time dependent calculation. Auto generation of mesh is one of the very useful features of the modelling software and another attractive feature is colorful output of the graph and results.

Parise and Lollino (2011) observe in their model that natural caves represent a potential hazard for the built environment, due to the occurrence of instability within caves, which may propagate upward and eventually reach the ground surface, inducing the occurrence of sinkhole. They analyzed the failure mechanisms observed in the field for such underground instability processes and the factors that seem to influence the processes. Numerical analyses were done using both the distinct element method (DEM) for jointed rock mass conditions and the finite element method (FEM) for geological settings represented by continuous soft rock mass. Both the effects of local instability processes occurring underground and the effects of the progressive enlargement of the caves on the overall stability of the rock mass were investigated along with the consequent failure mechanisms.

2.5 Particle Flow Code in 2 Dimensions (PFC^{2D})

PFC^{2D} (Particle Flow Code in 2 Dimensions) developed by Itasca Consulting Group Inc. (2008). PFC^{2D} is a discontinuum code used in analysis, testing, and research in any field where the interaction of many discrete objects exhibiting large-strain and/or fracturing is required. Because PFC^{2D} is not designed to examine a particular type of problem, its range extends to any analysis that examines the dynamic behavior of a particulate system.

In PFC^{2D} materials may be modeled as either bonded (cemented) or unbounded (granular) assemblies of particles. Though the code uses circular particles by default, particle shape may be defined in a PFC^{2D} model through use of the built-in clump logic.

The efficient contact detection scheme and the explicit solution method ensure that a wide variety of simulations from rapid flow to brittle fracture of a stiff solid are modeled accurately and rapidly. All the equations used in PFC^{2D} are documented. The user has access (via the powerful built-in programming language, FISH) to almost all internal variables. The codes are not "black boxes," but open software that can be used with confidence.

PFC^{2D} uses an explicit solution scheme that gives stable solutions to unstable processes. It can describe non-linear behavior and localization with accuracy that cannot be matched by typical finite element programs. This makes PFC^{2D}, along with its three-dimensional counterpart PFC^{3D}, the only commercially available codes of their kind.

Li and Wang (2011) use Particle Flow Code to simulate the process of subsidence and to calculate the distribution of contact force and displacement of ore particles, which have a good consistency in comparison with the actual survey data in Shandong province. PFC^{2D} well simulates the process of the mine collapse. Particle flow method has unique advantages in the simulation of mechanical behavior of broken ore particles, in the mechanical analysis of collapse process and in the collapse displacement of ores. Discrete element modeling is employed for this study due to its advantages in analyzing large deformations and discontinuous processes.

Mcnearny and Barker (1998) compare physical and numerical models of the block-caving mining methods. PFC^{2D} program was used in an attempt to better

understand the deformations and flow within each of the physical models during the draw procedure. Bridging and interlocking of the blocks occurred in approximately the same places and similar times during the draw sequence. The results show that the draw down patterns and the rate of draw generated within the numerical models were very similar in development of the physical models. For the given cases of the physical model, the numerical model simulated the behavior of the physical model quite well. The only constraints that were placed on the numerical models were the initial boundary conditions of the physical models. By inspection, the overall shape and flow lines of both the numerical and physical models were extremely close in area removed and flow characteristics. The numerical results as reported in this study are the result of the internal algorithms of the PFC^{2D}softwere.

Numerical methods are different from the other methods in that the geotechnical aspects of the mine working can be taken into account. Among numerical techniques, Particle Flow Code (PFC) is the most suitable method for solving highly non-linear and large strain problems like subsidence phenomena by means of laboratory-scale models and the actual survey data (Li and Wang, 2011; Lisjak and Grasselli, 2014). Therefore, the code PFC which base on Distinct Element Method (DEM) and explicit solution technique was chosen for simulating the subsidence in this study.

CHAPTER III

PHYSICAL MODEL SIMULATIONS

3.1 Introduction

The objective of the physical model simulations in this study is to determine the maximum subsidence and trough width as a function of cavern width and cavern height under super-critical condition. This chapter describes method, equipment, and results of the simulations. Super-critical subsidence usually occurs where the overburden thickness is less than the width of the cavern or mined-out area. The shallow mining induces this type of subsidence can affect the ground surface substantially, especially in salt solution mining (brine pumping method). Collapse of cavern roof and overburden can occur when the subsidence reaches its super-critical condition, which is dictated by the cavern height. If the cavern height is equal to or less than the roof deformation, the immediate roof rock will touch the cavern floor. If the cavern height is however significantly greater than the critical roof deformation, failure of the cavern roof can occur under the super-critical condition (Hawkes, 2010 and Thongprapha et al., 2015). The failure can progress upward and leads to a sinkhole development.

3.2 Material property

Fine sand (Figure 3.1) is used as the test material to simulate overburden in the physical model. The mechanical properties (grain size distribution and shearing resistance) for the tested material are obtained from those tested by Thongprapha et al.

(2015). The grain size analysis and calculation follow the ASTM D422-63 standard practice. The material has particle diameter from 0.425 to 2.36 mm, with more than 65.20% of 2 mm diameter (Figure 3.2). The sand is classified as poorly graded in accordance with ASTM D2487-06. The direct shear test is performed to determine the cohesion and friction of sand by used ASTM D5607-07 standard practice. The peak and residual shear strengths as a function of the normal stress of sand is shows in Figure 3.3. The properties of fine sand are shown in Table 3.1.

Figure 3.1 Clean and uniform sand with nominal sizes of 2 mm used to simulate overburden.

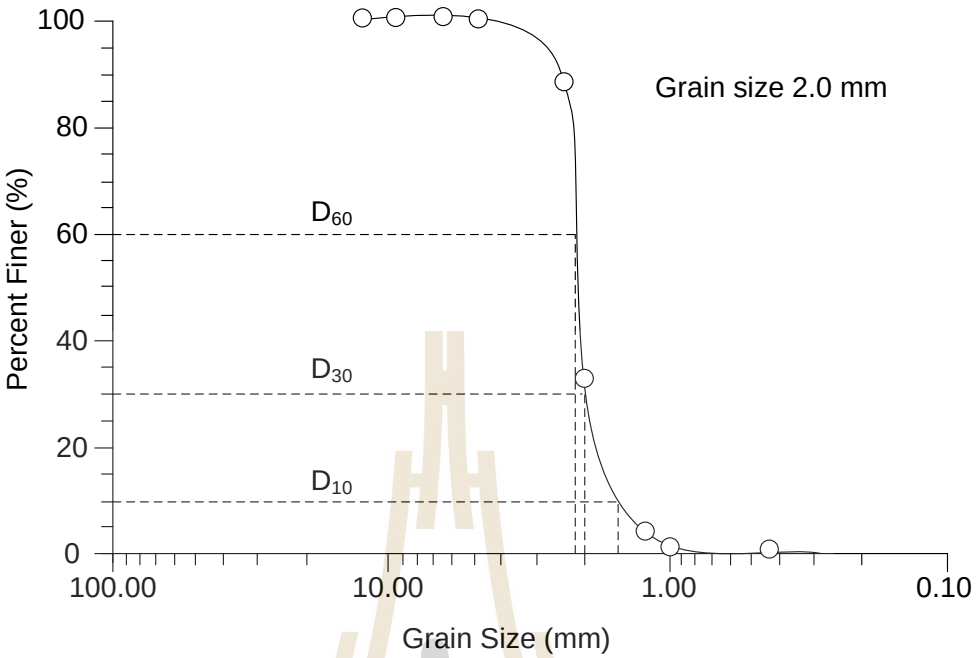

Figure 3.3 Grain size distribution curve of fine sand (Thogprapha et al., 2015).

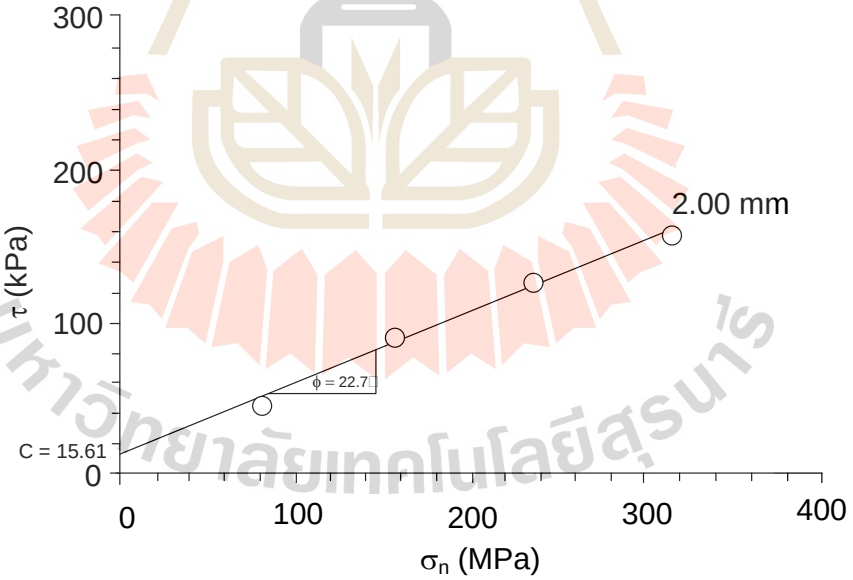

Figure 3.3 Shear strength as a function of normal stress obtained from direct shear testing (Thogprapha et al., 2015).

Table 3.1 Physical mechanical properties of fine sand (Thongprapha et al., 2015).

Test method	Soil properties		Values
Grain size Analysis	Uniformity coefficient, C_u		1.29
	Coefficient of curvater, C_c		1.07
	Type of soil		Poorly-graded sand
	Grain Shape	Sphericity	High sphericity
		Roundness	Subangular
Direct shear test	Bulk density (kN/m^3)		1455
	Cohesion, c (kPa)		15.61
	Friction angle, ϕ (degree)		22.7
	Normal stiffness, K_n (GPa/m)		44.54
	Shear stiffness, K_s (GPa/m)		0.73

3.3 Physical model testing

A trap door apparatus developed by Thongprapha et al. (2015) is used in the physical model simulations, as shown in Figure 3.4. The functions of the test frame are: (1) to simulate subsidence of overburden in three-dimension, (2) to assess the effect of overburden properties and the geometries of underground openings on the surface subsidence, and (3) to induce subsidence of overburden using the real gravitational force. The testing space is 95×95×60 cm^3. The measurement system of the surface subsidence includes a sliding rail with a laser scanner to measure the surface subsidence under various underground cavern geometries. The laser scanner can be moved

horizontally in two directions. For each simulated condition, the sample container is filled with the sand to a pre-defined thickness which represents thickness of overburden.

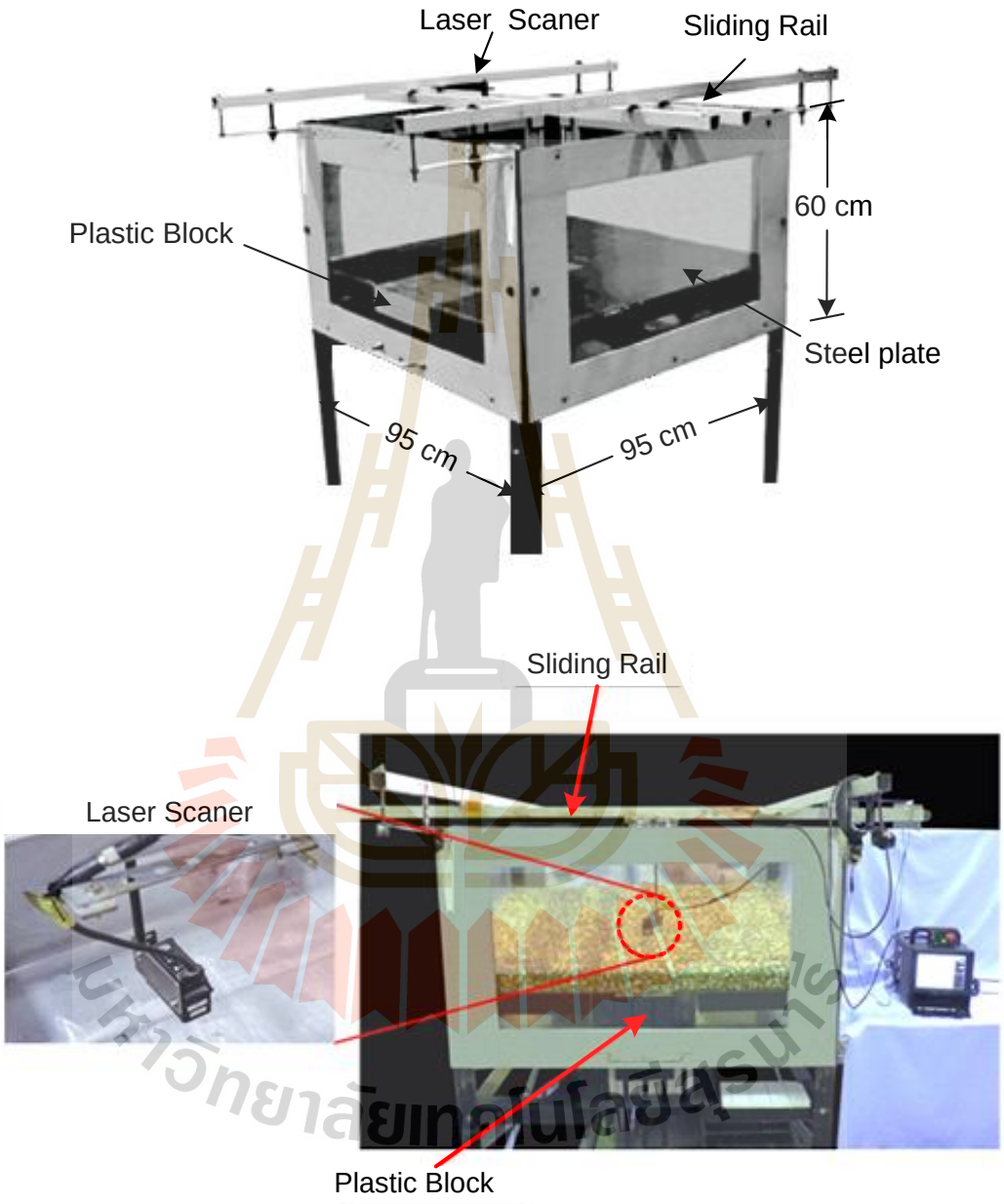

Figure 3.4 Trap door apparatus (Thongpraoha et al., 2015).

The sand is lightly packed, and the top surface is flattened before starting the simulation or test. The underground opening is simulated by carefully pulling down

the plastic blocks underneath the sample container. The opening width (W) is selected from 10, 30 to 50 mm. The opening length (L) is maintained constant at 200 mm. The opening height (H) is varied from 25, 50, 75 to 100 mm. The overburden thickness or opening depth (Z) is from 100 to 300 mm with 50 mm interval. Figure 3.5 shows the test parameters and variables defined in the physical model simulations.

After the underground opening is created, the settlement of the top surface occurs. The laser scanner measures the surface profile of the top surface of fine sand before and after the subsidence is induced. The measurements are made to the nearest 0.01 mm. The laboratory testing gives the maximum surface subsidence (S_{max}) and the trough width (B). The point of maximum surface subsidence is located at the point of the maximum subsidence trough. The trough width is measured from the point of surface subsidence to the point of zero surface subsidence.

An example of a scanned image in three dimensions is shown in Figure 3.6. Figure 3.7 shows an example of 2-D laser scanned profile. The physical model results are focused on the variation of the maximum surface subsidence (S_{max}) and subsidence trough width (B) as affected by the opening geometry, and block size under super critical condition. Each opening configuration is simulated at least 3 times to verify the repeatability of the results.

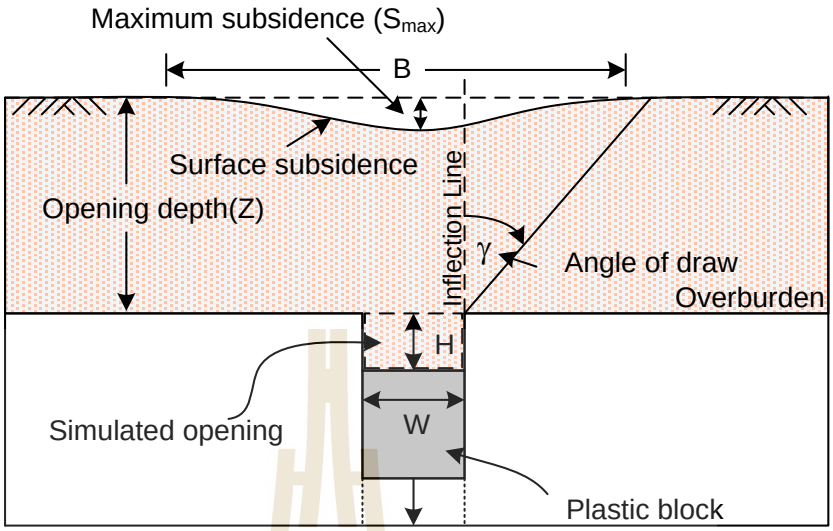

Figure 3.5 Variables used in physical model simulations.

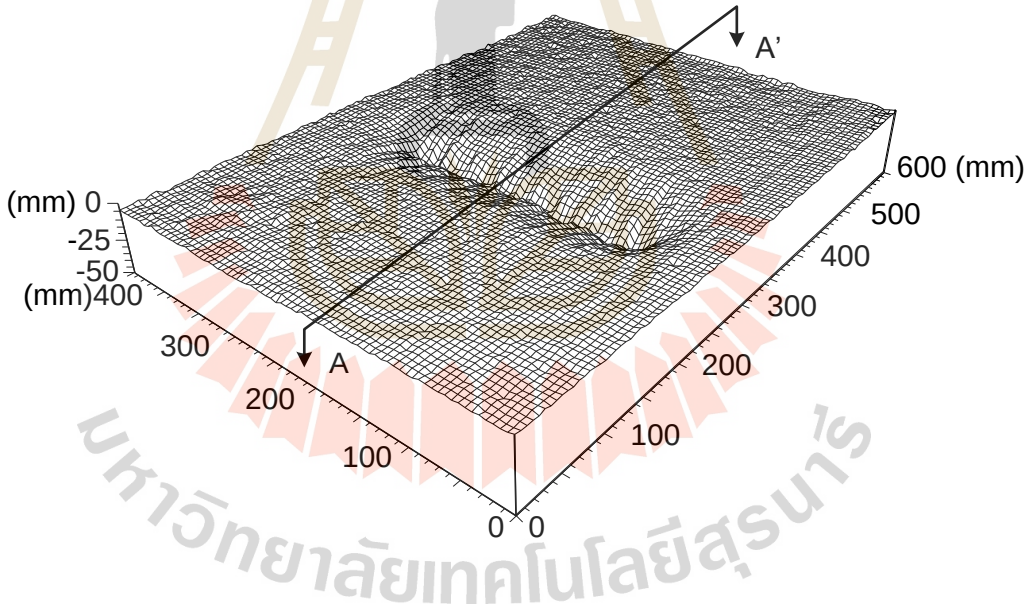

Figure 3.6 Example of three-dimensional laser scanned image of subsidence of sand overburden.

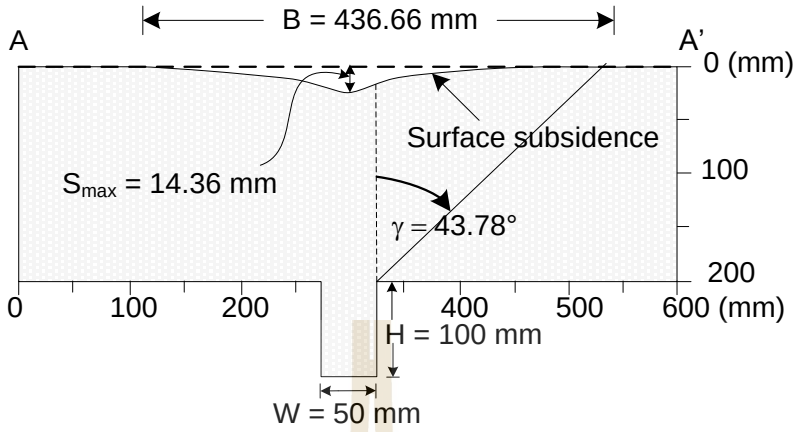

Figure 3.7 Example of cross-section (A-A') of surface subsidence profiles.

3.4 Test results

The measurement results obtained here are shown in Table 3.2, presented in terms of the maximum subsidence (S_{max}), trough width (B) and angle of draw (γ). Line scanned profiles of sand subsidence are shown in Figures 3.8 through 3.12. The maximum subsidence measurements (S_{max}) as a function of the opening height (H) for each opening width (W) are shown in Figure 3.13. The results clearly indicate that the maximum subsidence increases with increasing opening height and opening width. This is because the particles can collapse into the opening more when the volume of opening becomes larger. The maximum subsidence tends to decrease slightly as the overburden thickness increases, particularly for opening width equal to 10 mm. This is because of the inter–locking of fine sand particles above the opening (Meguid et al., 2008). This observation agrees well with those of Thongprapha et al. (2015) who study the surface subsidence above underground opening using gravel in order to exhibit a cohesionless frictional behavior of the overburden material. Note that the S_{max} values

are more sensitive to the opening height for the wide openings than for the narrow ones (Figure 3.13).

The trough widths (B) as a function of opening width are given in Figure 3.14. The trough width increases with increasing opening height and opening width. This is simply because under super-critical conditions, the material can collapse (flow) into the opening more easily, and hence induces larger trough width. These results agree with the conclusion drawn by Thongprapha et al. (2015) and Saoanunt and Fuenkajorn (2015) that the subsidence area and maximum subsidence are controlled by the geometrical characteristics of underground openings, overburden thickness, and mechanical properties of the overburden. The angle of draw (the extent of the subsidence affected area) increases with increasing opening length (L) as a function of opening width (W) ratio.

The test results in Figures 3.13 and 3.14 indicate that the increase of maximum subsidence closely relates to the increase of opening height, while the increase of trough widths is related to the increase of opening width. The S_{max} values tend to be independent of the opening depths or overburden thickness. The trough width however is more sensitive to the overburden thickness. This agrees with the postulation given by Singh (1992) that under super-critical subsidence condition the maximum subsidence tends to be constant, while the trough width tends to increase with the opening width.

Table 3.2 Physical model test variables and results.

Test variable			Results		
Z (mm)	**W (mm)**	**H (mm)**	**S_{max} (mm)**	**B (mm)**	**γ (degrees)**
100	10	100	4.50	120.66	29.11
		75	2.70	105.03	25.42
		50	2.10	101.04	24.53
		25	1.08	93.83	23.18
	30	100	9.88	220.30	43.62
		75	7.00	194.07	39.37
		50	3.60	160.12	33.07
		25	2.15	143.56	29.49
	50	100	12.83	278.63	48.65
		75	10.80	259.39	46.23
		50	6.70	218.61	40.13
		25	3.22	180.59	33.14
150	10	100	3.20	140.97	23.74
		75	2.60	139.10	23.14
		50	1.56	124.01	20.80
		25	1.05	110.42	18.50
	30	100	9.95	280.82	39.88
		75	5.15	229.04	33.43
		50	2.90	199.08	29.27
		25	1.32	168.93	24.85
	50	100	14.58	374.06	47.21
		75	8.90	306.92	40.58
		50	4.31	250.92	33.81
		25	2.28	215.66	29.03
200	10	100	2.50	165.90	21.22
		75	1.50	161.24	20.71
		50	0.80	134.42	17.28
		25	0.68	130.38	16.80
	30	100	9.60	336.00	37.42
		75	5.60	289.06	32.93
		50	2.80	250.38	28.85
		25	1.22	212.72	24.55

Table 3.2 Physical model test variables and results (Cont.).

Test variable			Results		
Z (mm)	**W (mm)**	**H (mm)**	**S_{max} (mm)**	**B (mm)**	**γ (degrees)**
200	50	100	14.36	436.66	43.78
		75	9.00	372.94	38.92
		50	3.90	300.08	32.01
		25	1.82	259.42	27.63
250	10	100	2.20	180.00	18.78
		75	0.80	162.00	16.91
		50	1.08	146.93	15.31
		25	0.88	125.00	12.95
	30	100	8.50	361.00	33.50
		75	4.53	314.00	29.60
		50	2.50	285.00	27.02
		25	0.70	229.00	21.70
	50	100	13.50	462.00	39.49
		75	7.90	415.00	36.13
		50	4.25	369.00	32.54
		25	1.20	290.85	25.72
300	10	100	1.50	174.99	15.38
		75	0.54	129.90	11.30
		50	0.36	76.68	6.34
		25	0	0	0
	30	100	6.00	400.89	31.72
		75	3.51	357.57	28.63
		50	1.80	313.68	25.30
		25	0.06	250.95	20.22
	50	100	12.09	539.49	39.21
		75	6.90	459.96	34.34
		50	3.60	396.99	30.04
		25	0.99	320.76	24.29

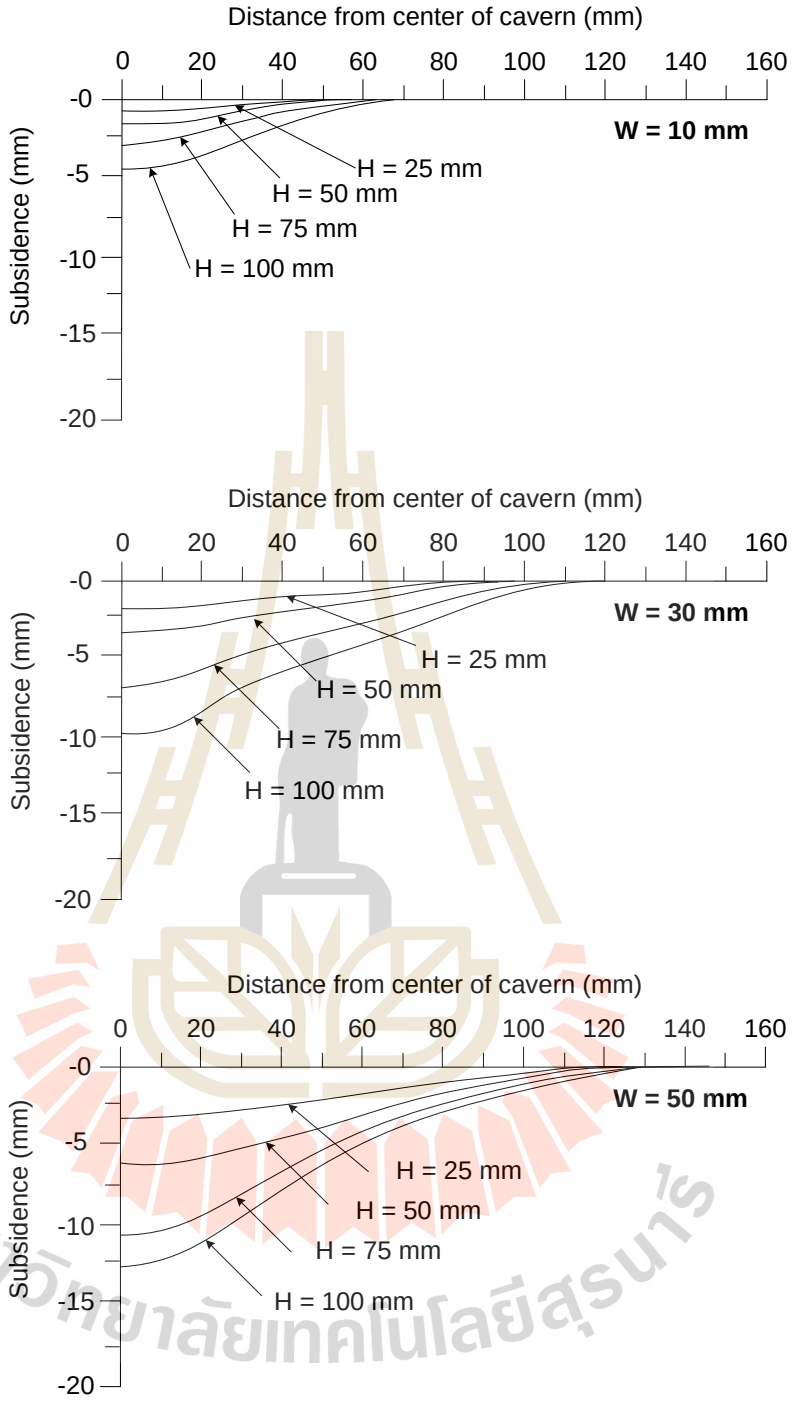

Figure 3.8 Line scanned profile of surface subsidence for overburden thickness (Z) 100 mm in each opening height (H) and opening width (W). Note that vertical scale is exaggerated to enhance the subsidence profile.

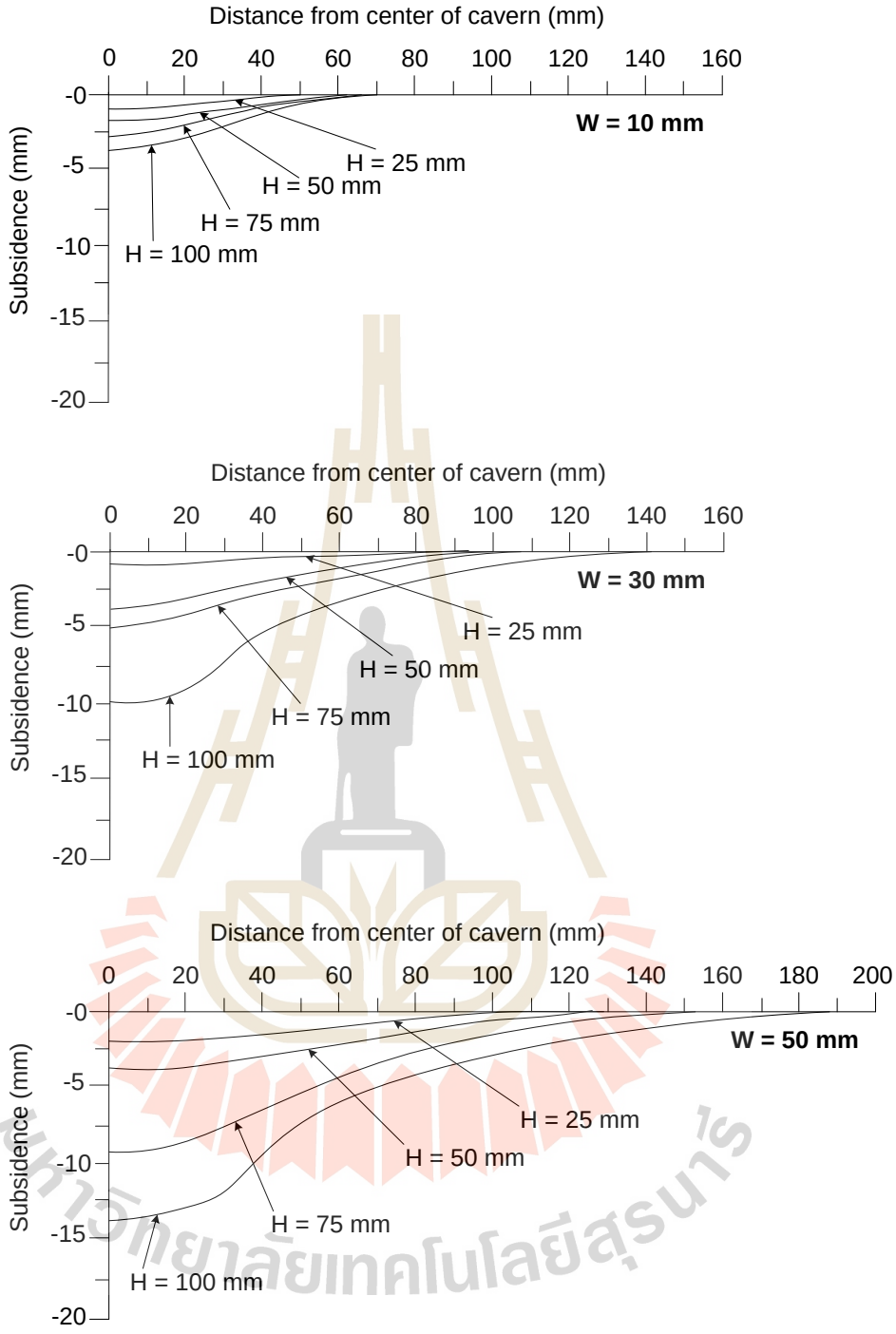

Figure 3.9 Line scanned profile of surface subsidence for overburden thickness (Z) 150 mm. Note that vertical scale is exaggerated to enhance the subsidence profile.

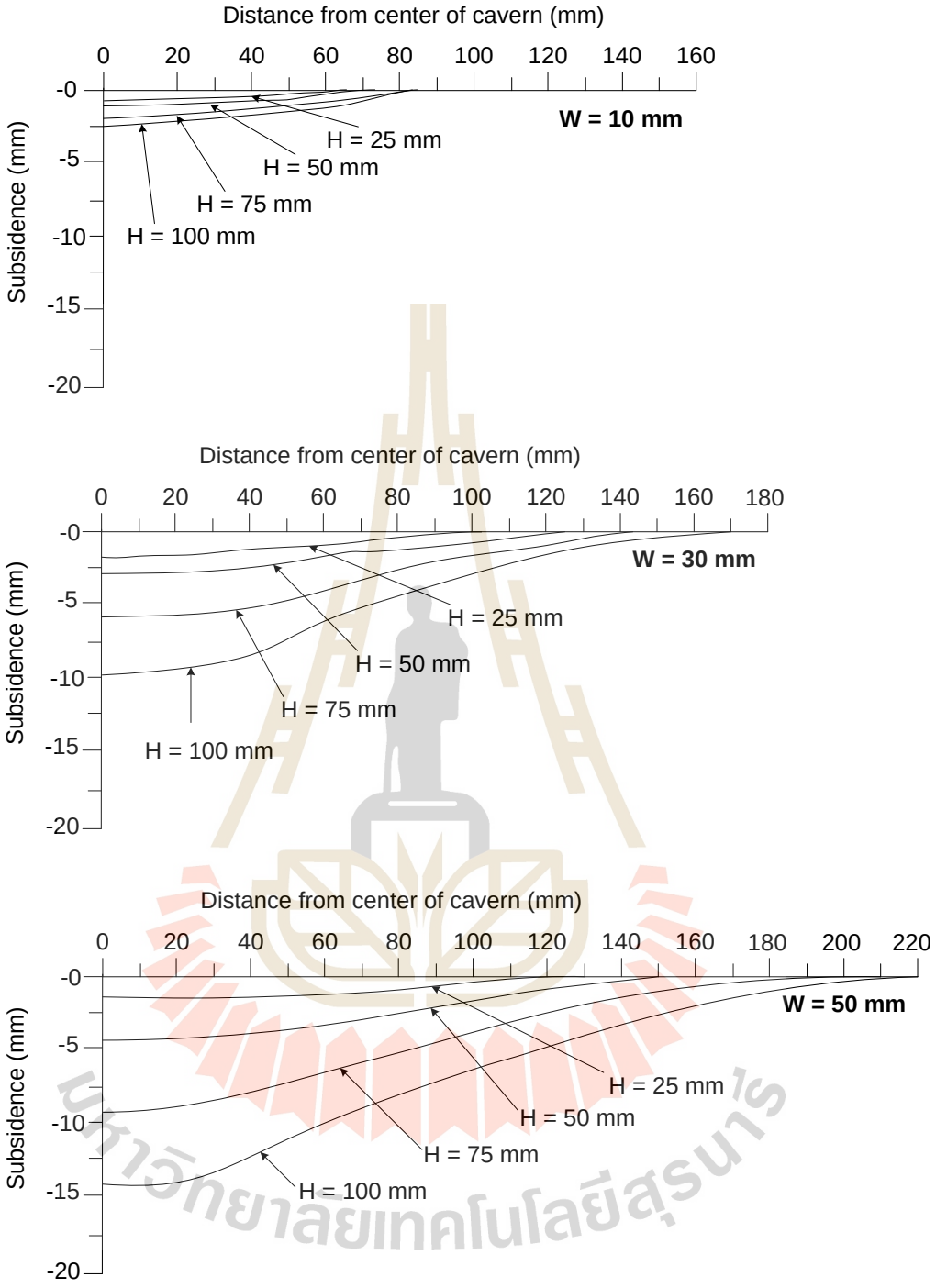

Figure 3.10 Line scanned profile of surface subsidence for overburden thickness (Z) 200 mm. Note that vertical scale is exaggerated to enhance the subsidence profile.

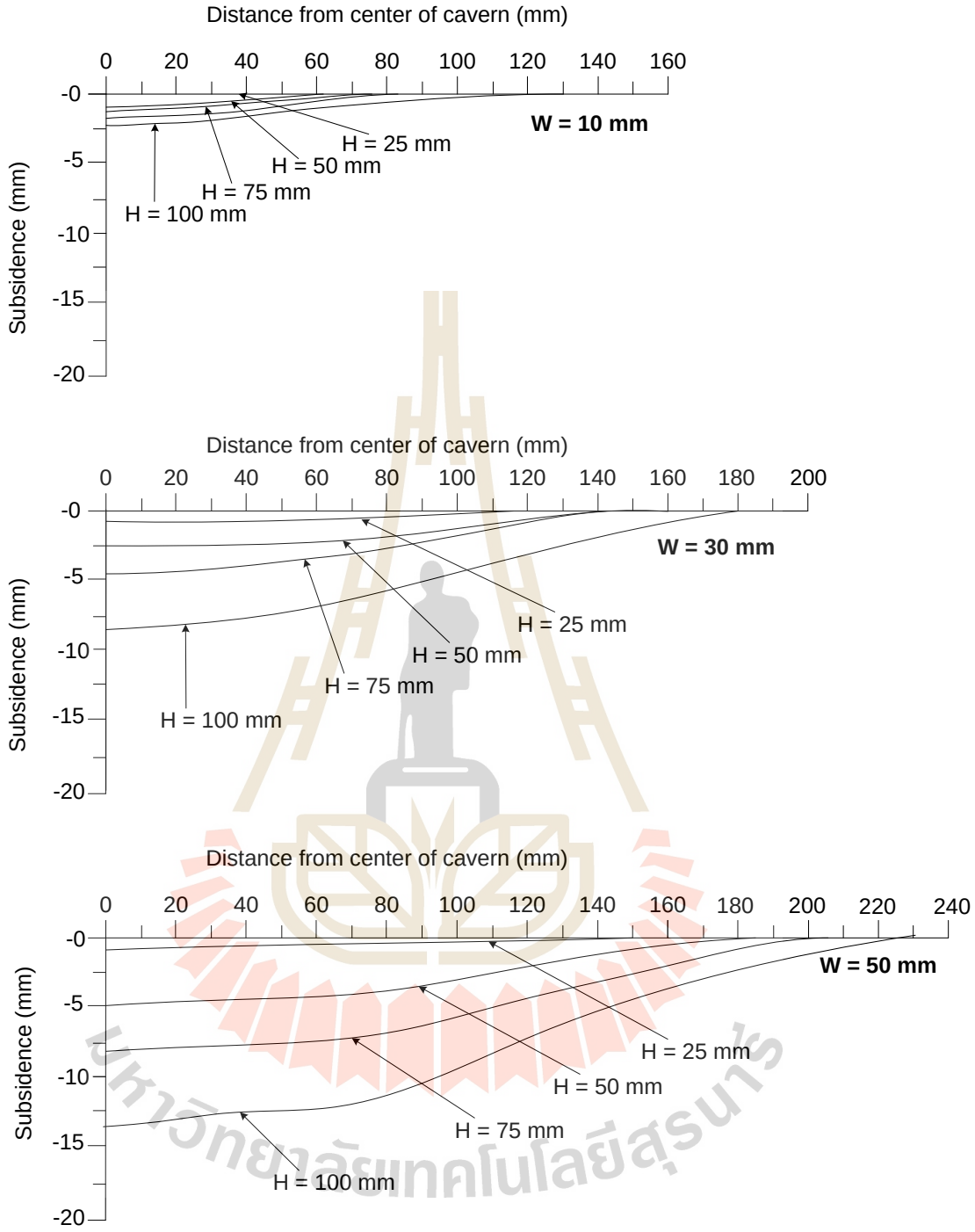

Figure 3.11 Line scanned profile of surface subsidence for overburden thickness (Z) 250 mm. Note that vertical scale is exaggerated to enhance the subsidence profile.

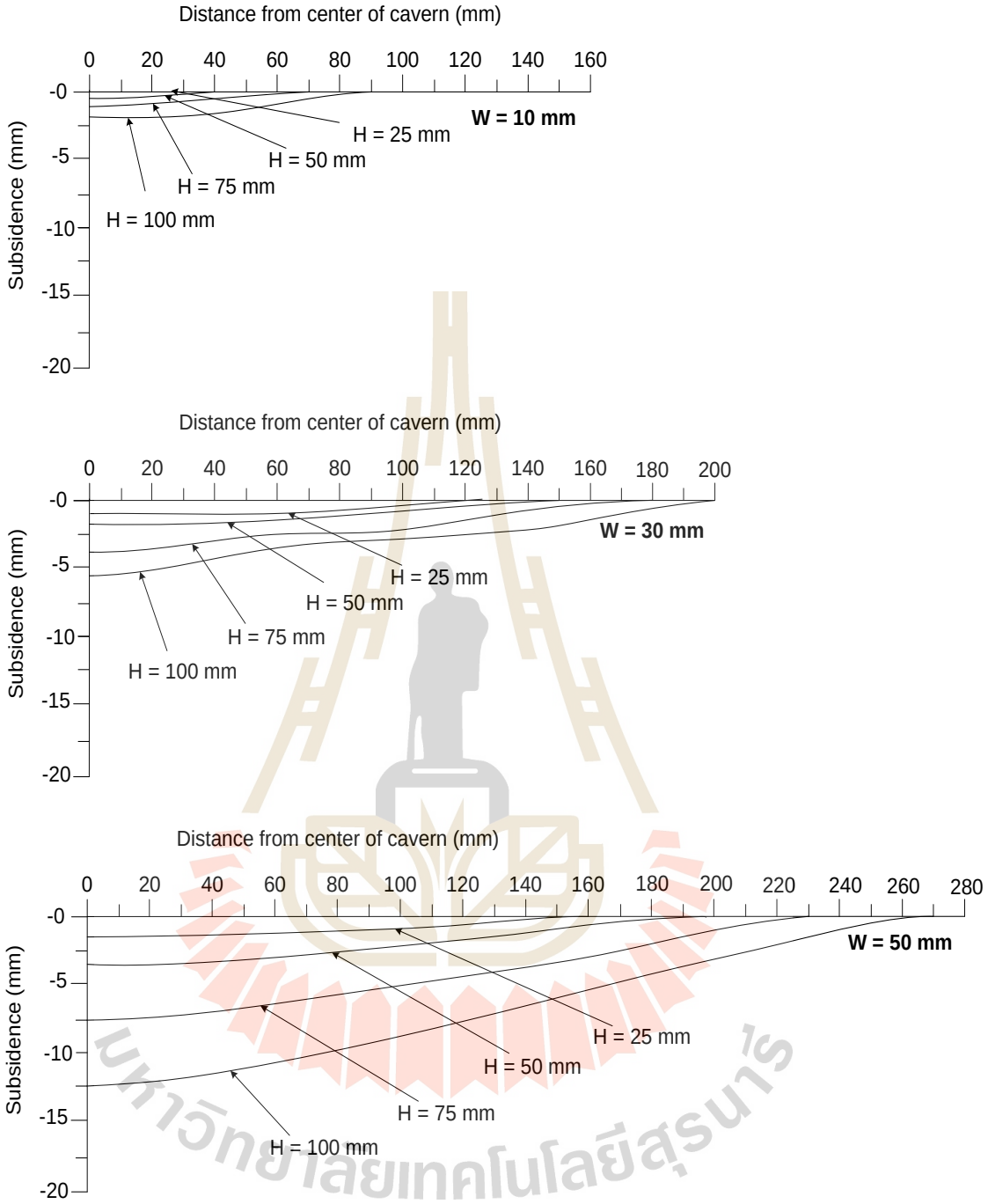

Figure 3.12 Line scanned profile of surface subsidence for overburden thickness (Z) 300 mm. Note that vertical scale is exaggerated to enhance the subsidence profile.

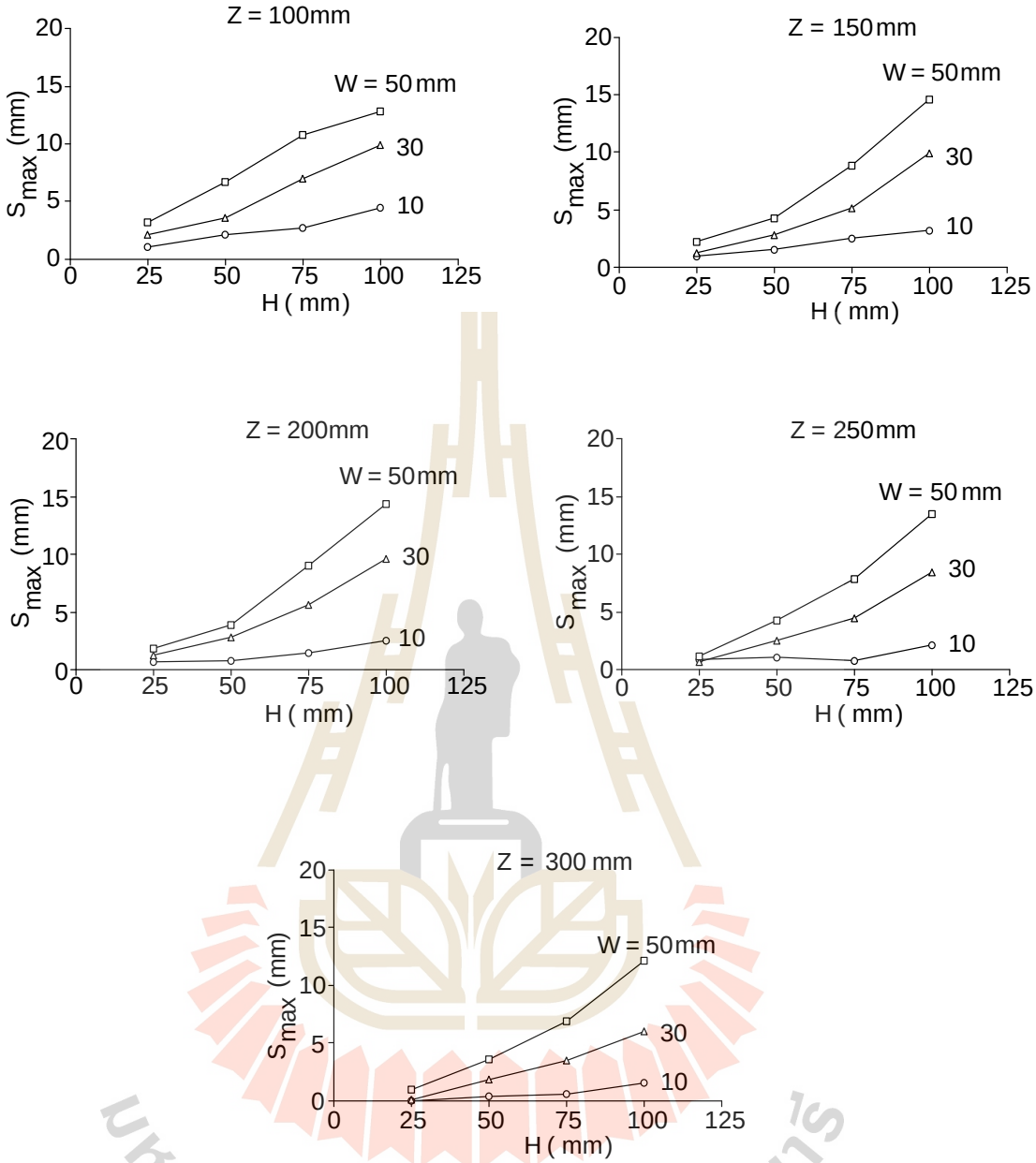

Figure 3.13 Maximum subsidence (S_{max}) as a function of opening height (H).

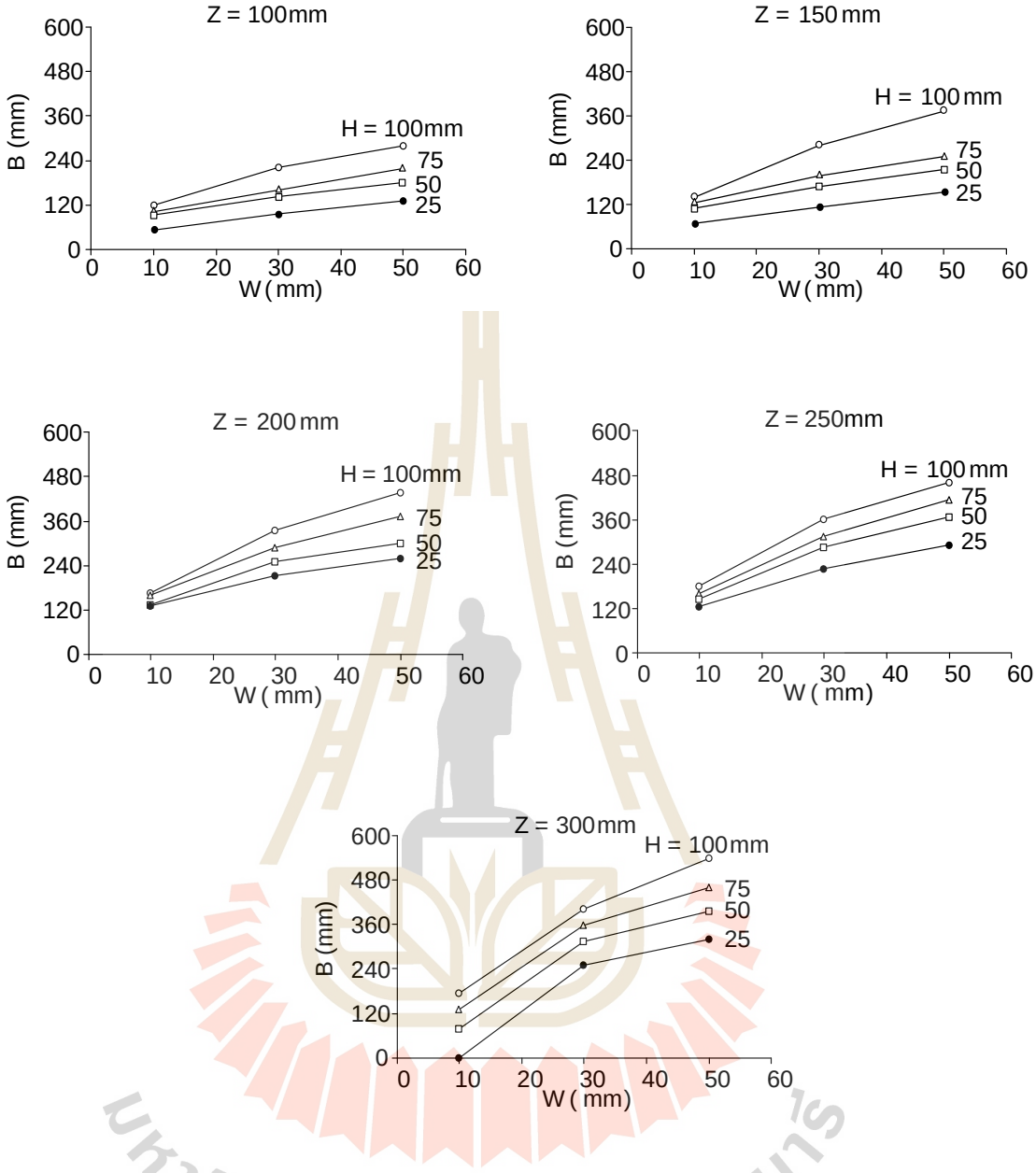

Figure 3.14 Trough width (B) as a function opening width (W).

CHAPTER IV

NUMERICAL SIMULATIONS

4.1 Introduction

This chapter describes the discrete element analyses using Particle Flow Code in two Dimensions (PFC^{2D}-Itasca, 2008) to compare the results with those of the physical model. The primary objectives are to verify the physical model results and to allow extrapolating the numerical model results to the conditions beyond those used in the physical modeling. The model simulations and results are presented. The calculations of surface subsidence in difference friction angle using are also made.

4.2 Particle Flow Code in two Dimensions (PFC^{2D}) Simulations

PFC has been extensively used within the rock mechanics community to numerically investigate the fundamental processes of brittle fracturing in rocks by means of laboratory-scale models. PFC^{2D} simulates the movement and interaction of circular particles by the distinct element method (DEM). Particle-based models were originally developed to simulate the mechanical behavior of non-cohesive media, such as soils and sands (Cundall and Strack, 1979). With this approach the granular structure of the material is modeled as a statistically generated assembly of rigid circular particle. The contacts between particles are typically assigned normal and shear stiffnesses as well as coeffient. The force arises from the weight of the particle and from the contact force between particles

(Bobet, 2010). The calculation is carried out with PFC^{2D} code (Itasca, 2008) which is based on Distinct Element Method (DEM) and it can be performed in following 5 steps:

1. Determination of material behavior model and material properties.
2. Formation of the model geometry.
3. Determination of the boundaries and initial condition; initial running of the program and monitoring of the model response.
4. Re-evaluation of the model and necessary modifications.
5. Interpretation of the result.

The discrete element analyses using PFC^{2D} (Itasca, 2008) are performed to correlate the results with those of the physical models and simulated the surface subsidence in difference friction angles of overburden.

4.2.1 Test Parameters

The parameters used in the PFC^{2D} model are identical to those of the physical model tests. The properties of the underground opening and sand overburden are given in Chapter III. Some important parameters for the simulations of subsidence are:

- particle radius is 1 mm,
- friction angle is 22.7 degree,
- bulk density is 1,455 kN/m^3,
- friction coefficient is 0.46,
- normal stiffness (K_n) is 44.54 GPa/m,
- shear stiffness (K_s) is 0.73 GPa/m, and
- cohesion is taken as zero for all cases (cohesionless material)

Several friction angles are assumed varying from 20, 25, 30, to 35 degrees. The assumption of zero cohesion used here is also supported by the experimental results of Barton (1974), Crosby (2007) and Grøneng et al. (2009) who found that the cohesion of rock mass comprising claystone, mudstone and siltstone is zero or negligible. The boundary conditions defined in the PFC^{2D}, are similar to those used in the physical models.

4.2.2 Discrete Element Analyses

The walls are generated in order to be used to simulate the boundary conditions of the overburden and the underground opening. All walls of the models are considered smooth and nonrestrictive with regards to material movement. The boundary conditions used in the simulation are identical to those of the physical model tests. The generated command places particles within the boundary specified such that no overlap occurs. The tries keyword specified 500,000 – 1,500,000 attempts to add the desired number of particles within the defined area. It simply creates the desired underground mining region and increases the number of tries to fit all of the particles within the specified area. This method is slow to achieve the initial equilibrium state, since particles move to large distances to come to rest. Once all of the particles are at rest and the model is at equilibrium, the top of the particle assembly is leveled by deleting all particles above a specified thickness of overburden (Figure 4.1). The command codes define the generation of the overburden model and the boundaries, as well as perform the extraction operations similar to those in the physical models. Each particle is assigned by the same property as those of the physical granular materials.

After the particles are at rest and the model is at equilibrium as predefined overburden thickness, the wall above the opening (roof) is deleted to

simulate the solution cavern (extraction) of material from each case using the equivalent procedures used in the physical model. The particles continuously flow into the opening floor until the opening completely fill, and hence the surface subsidence is induced (Figure 4.2). The subsidence of the overburden for both physical and numerical approaches, is governed by gravity. No lateral pressure is applied.

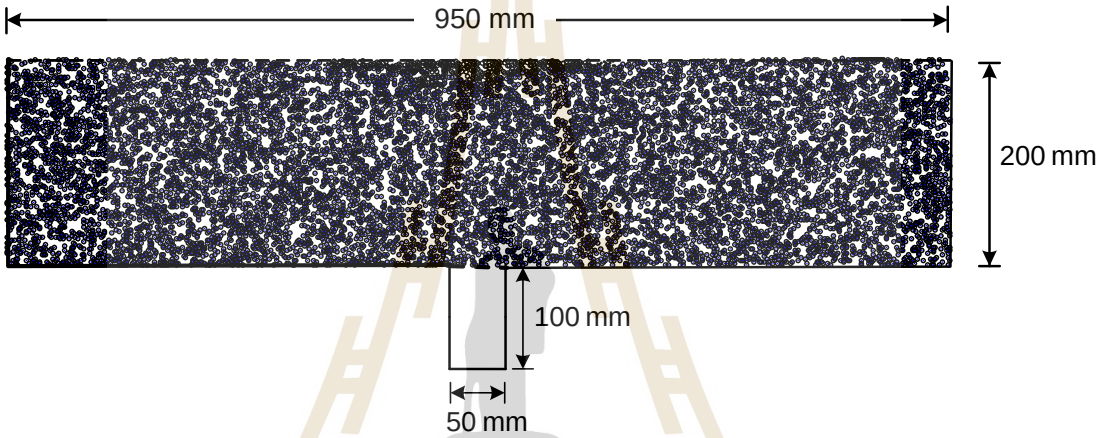

Figure 4.1 Example of surface subsidence before opening simulation with predefined overburden thickness.

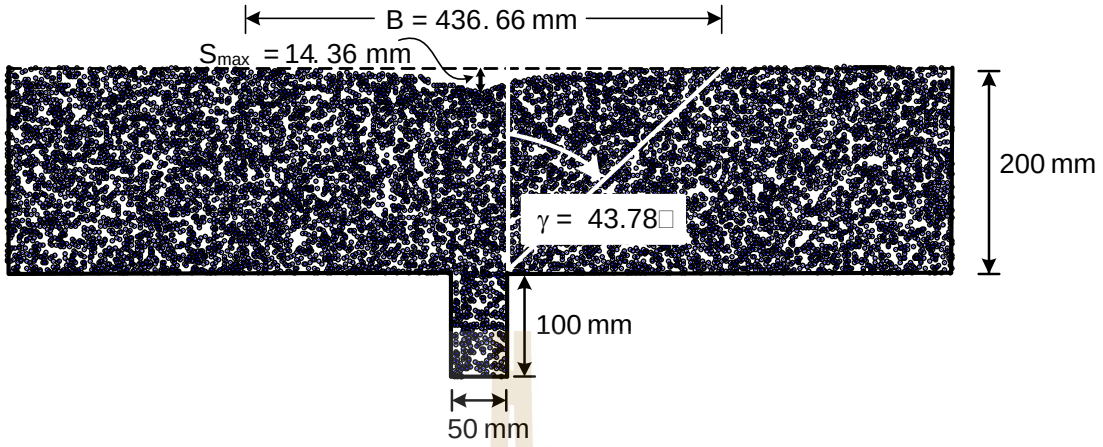

Figure 4.2 Example of PFC^{2D} model for surface subsidence after opening simulation.

4.3 Results

Figures 4.3 and 4.4 compare the physical model results with the PFC^{2D} simulations for friction angle of overburden equal to 22.7 degrees for different opening depths, opening height, and opening width. The maximum subsidence (S_{max}) as a function of opening height (H) is given in Figure 4.3, and the trough width (B) as a function of opening width (W) is given in Figure 4.4. Both approaches indicate that the S_{max} values tend to be independent of the opening depths. The trough width however is sensitive to the overburden thickness. The increase of the maximum subsidence closely relates to the increase of opening height, while the increase of trough width is related to the increase of opening width. The results from PFC^{2D} simulations agree well with those observed from the physical model testing. The close agreement between the numerical simulations and the physical model measurements suggests that the procedure and results of the physical modelling are accurate and reliable.

The results of friction angles varying from 20, 25, 30 to 35 degrees are presented in terms of the maximum subsidence (S_{max}) and trough width (B). Figures 4.5 through

4.8 show the maximum subsidence results and trough width for varied friction angles, as a function of opening height and opening width, respectively. The simulation results indicate that the maximum subsidence and trough width are decrease slightly with increasing friction angle of overburden material under the same opening geometry and overburden thickness.

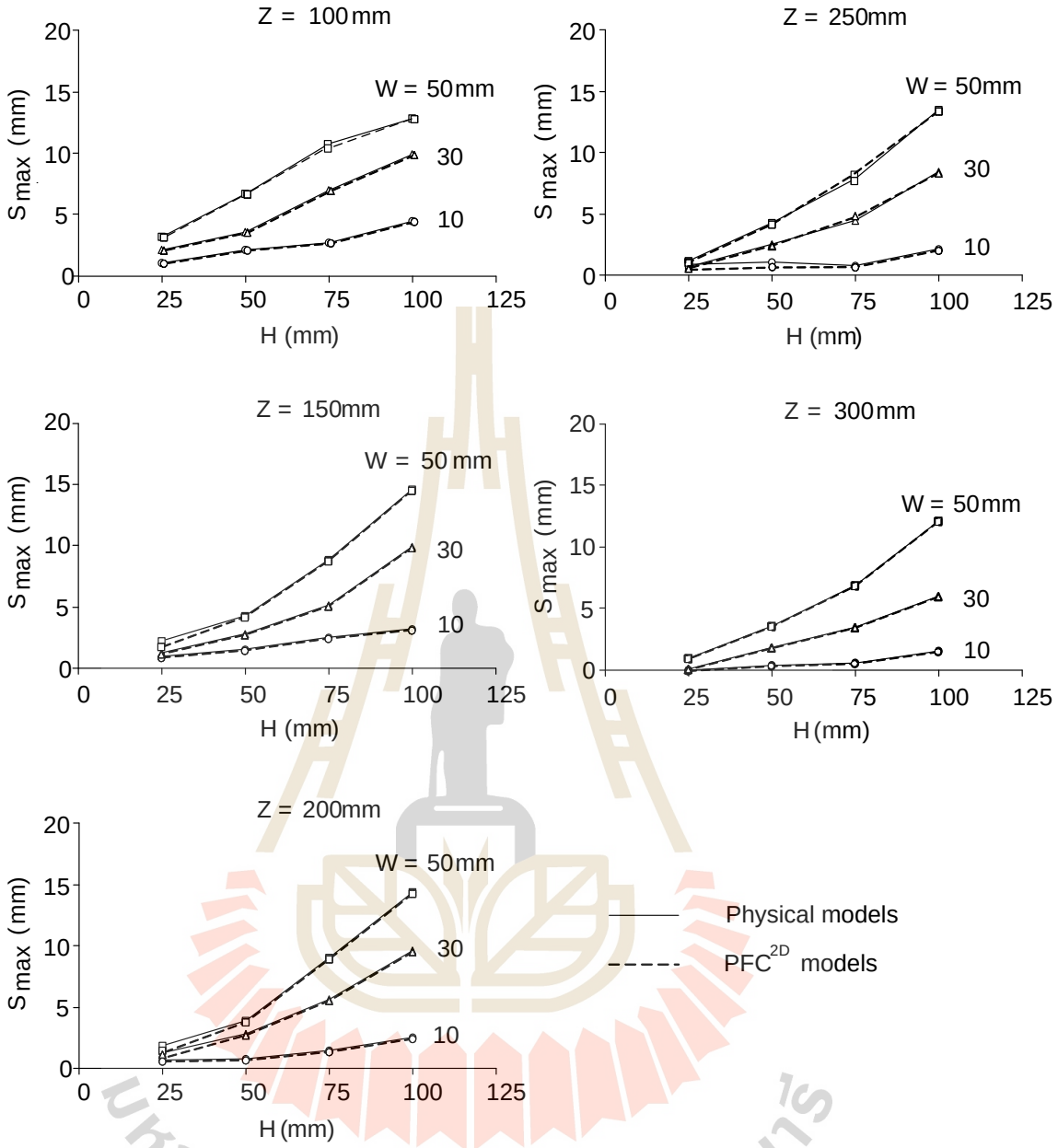

Figure 4.3 Comparisons of maximum subsidence (S_{max}) between physical model results (solid lines) and PFC model simulations (dash lines).

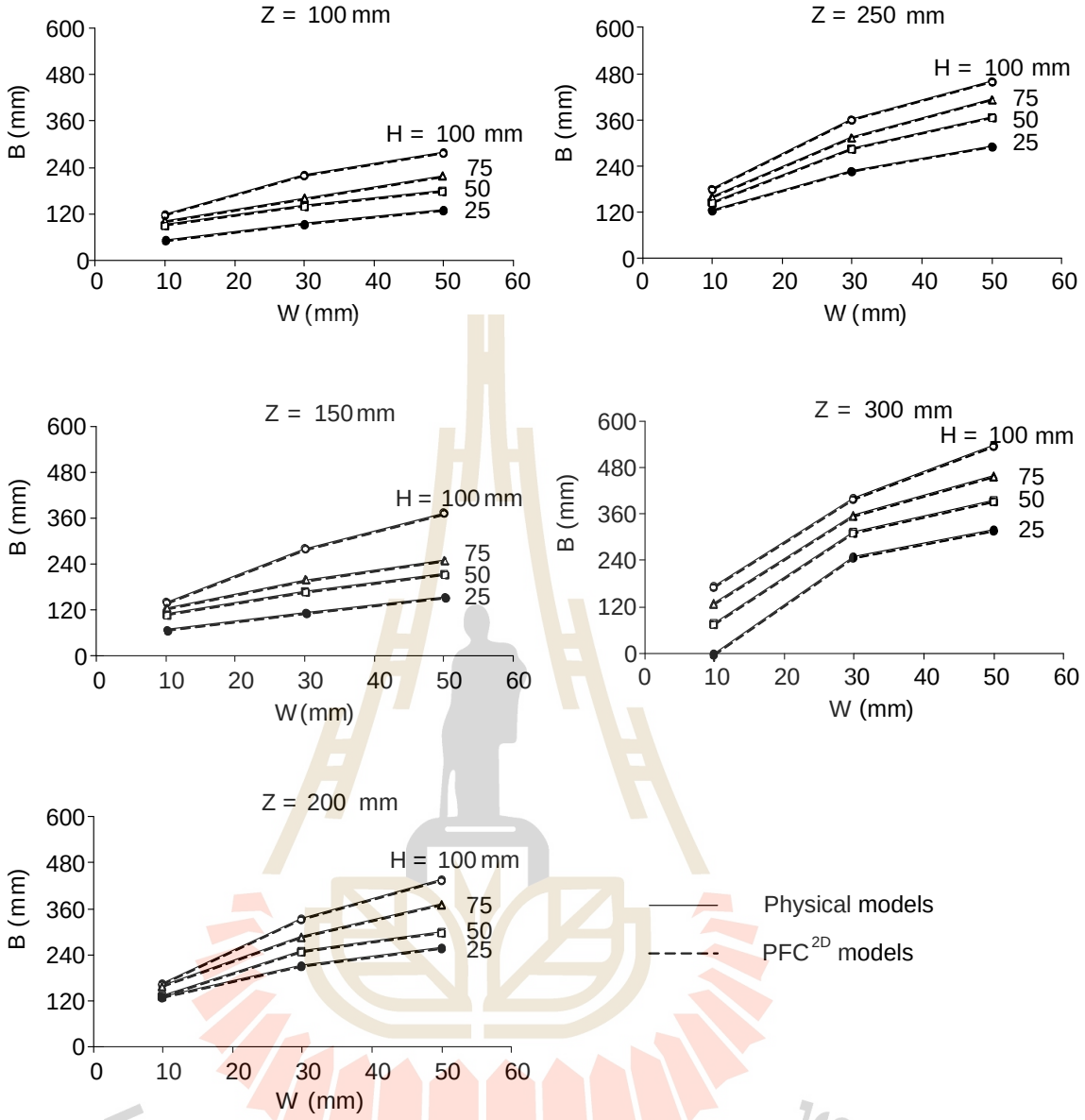

Figure 4.4 Comparisons of trough (B) between physical model results (solid lines) and PFC model simulations (dash lines).

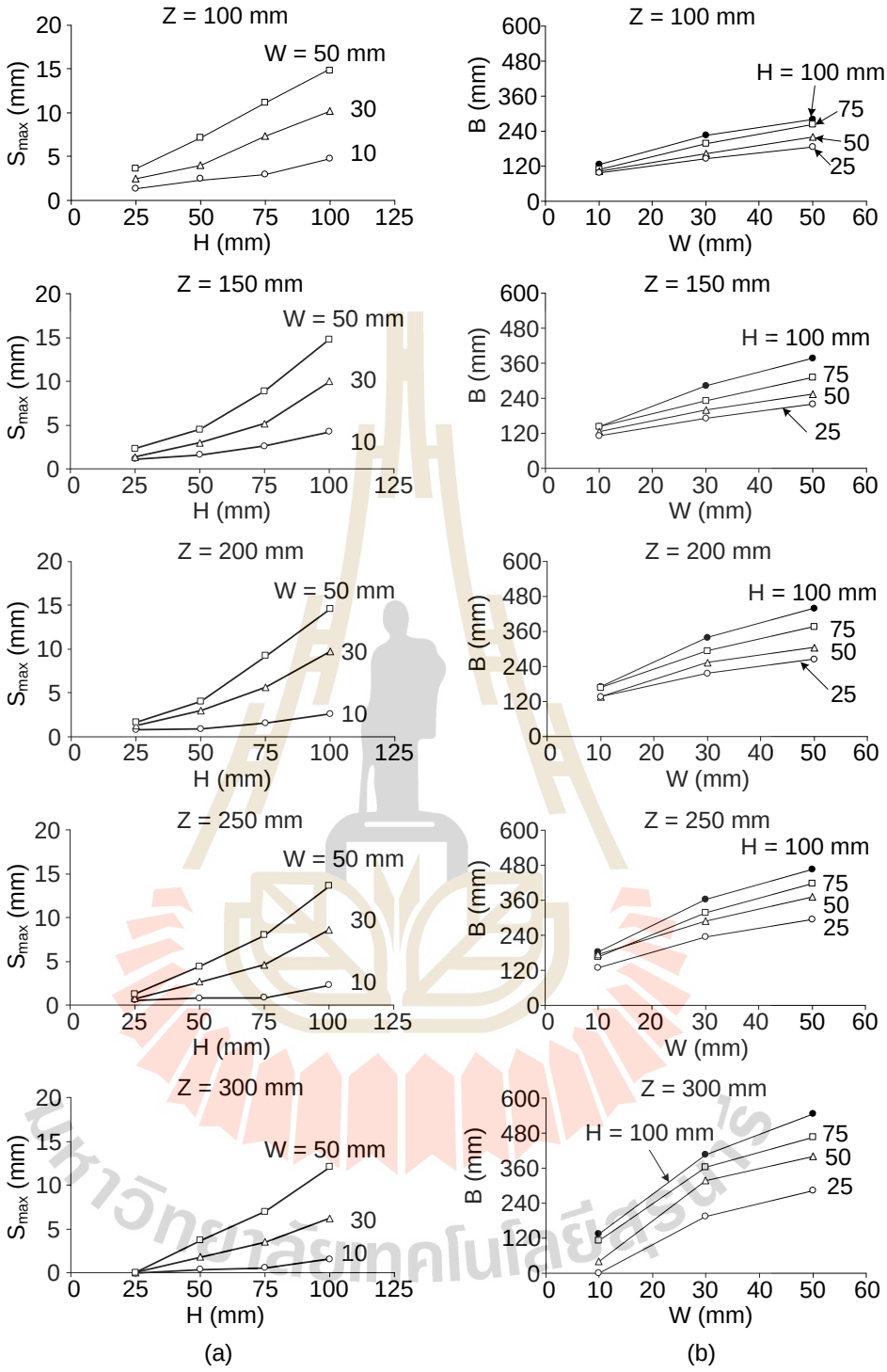

Figure 4.5 (a) Maximum subsidence (S_{max}) as a function of opening height (H), and (b) trough width (B) as a function of opening width (W) for friction angle of 20°.

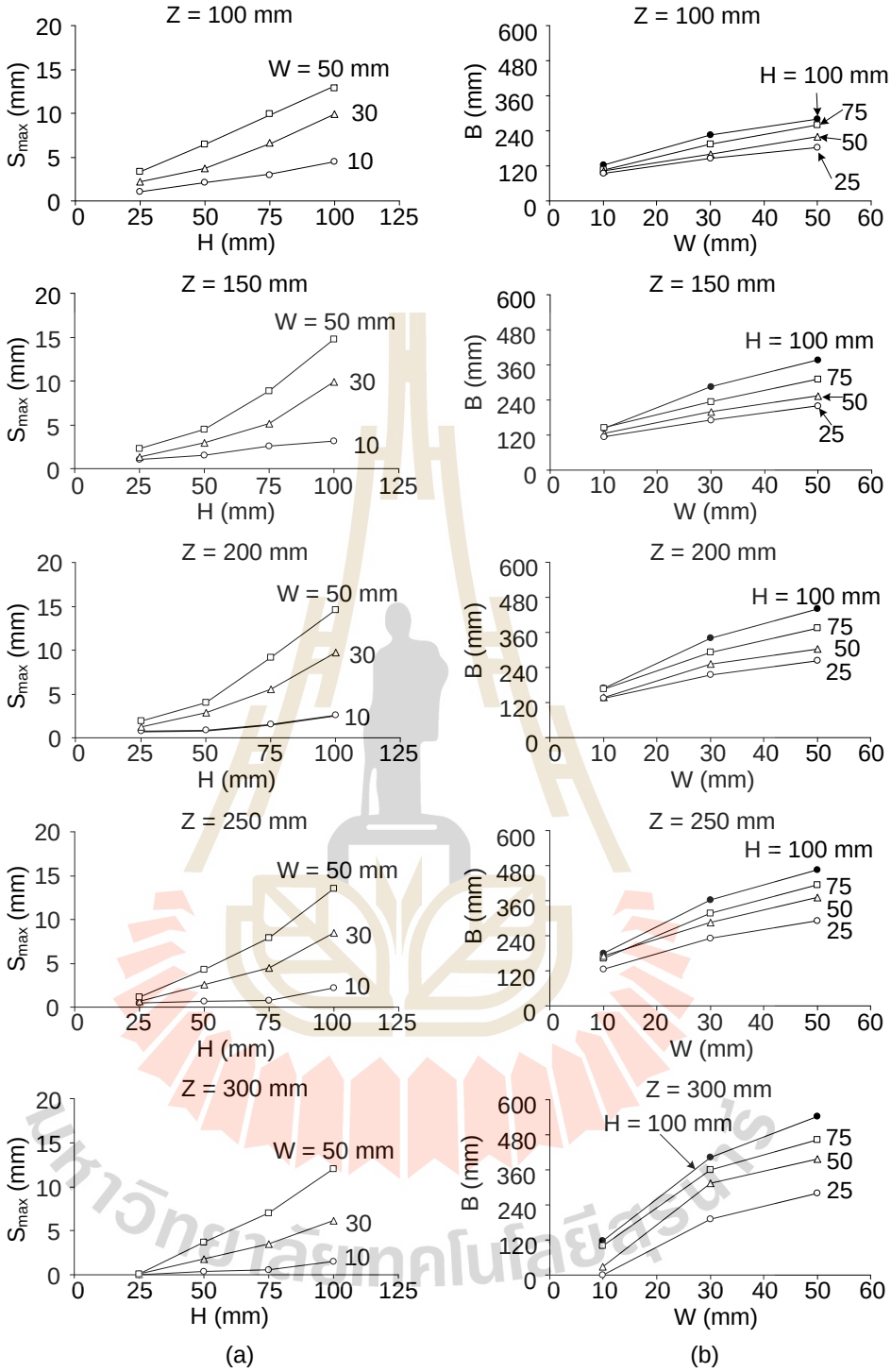

Figure 4.6 (a) S_{max} as a function of H, and (b) B as a function of W for friction angle of 25°.

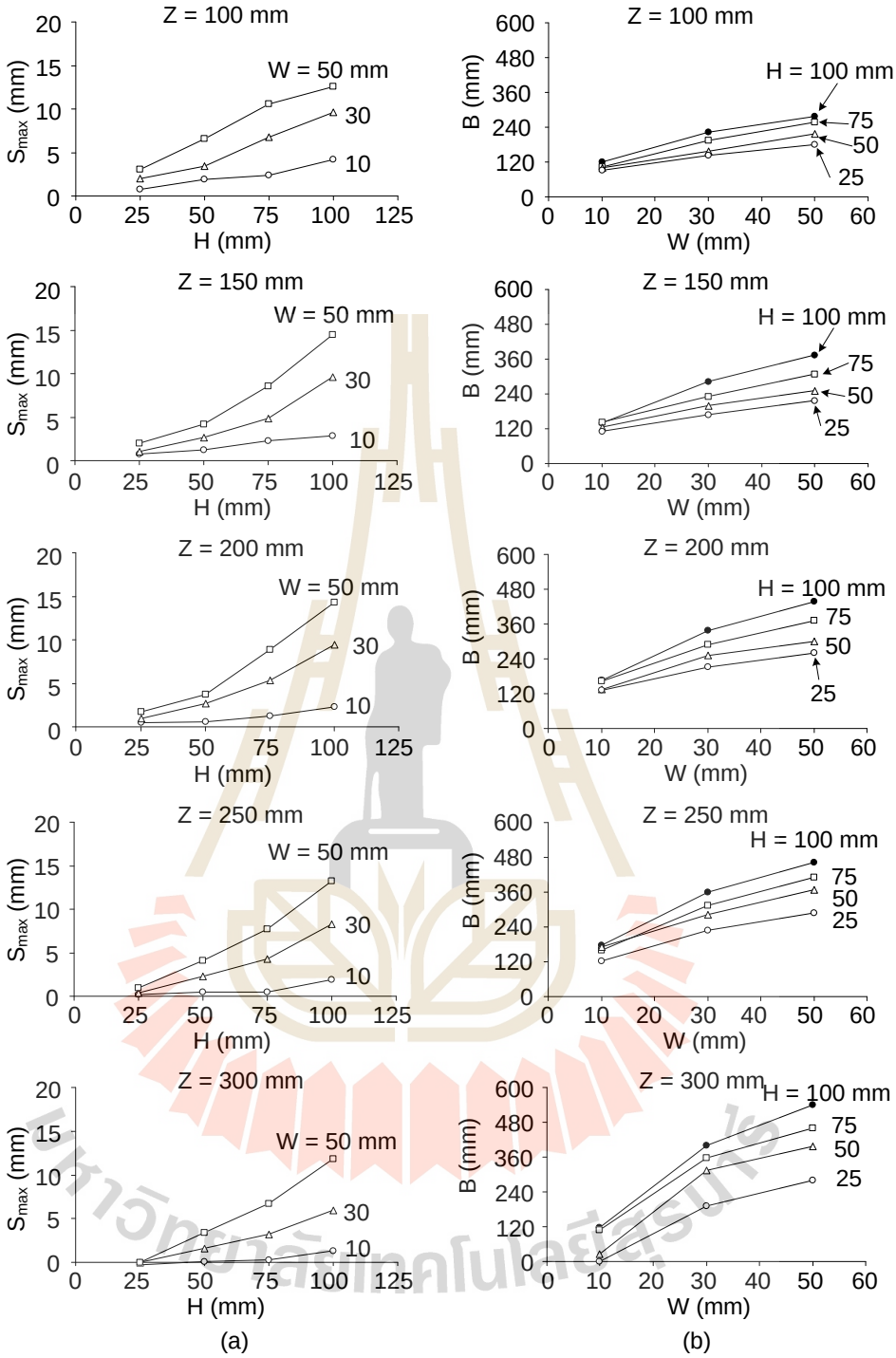

Figure 4.7 (a) S_{max} as a function of H, and (b) B as a function of W for friction angle of 30°.

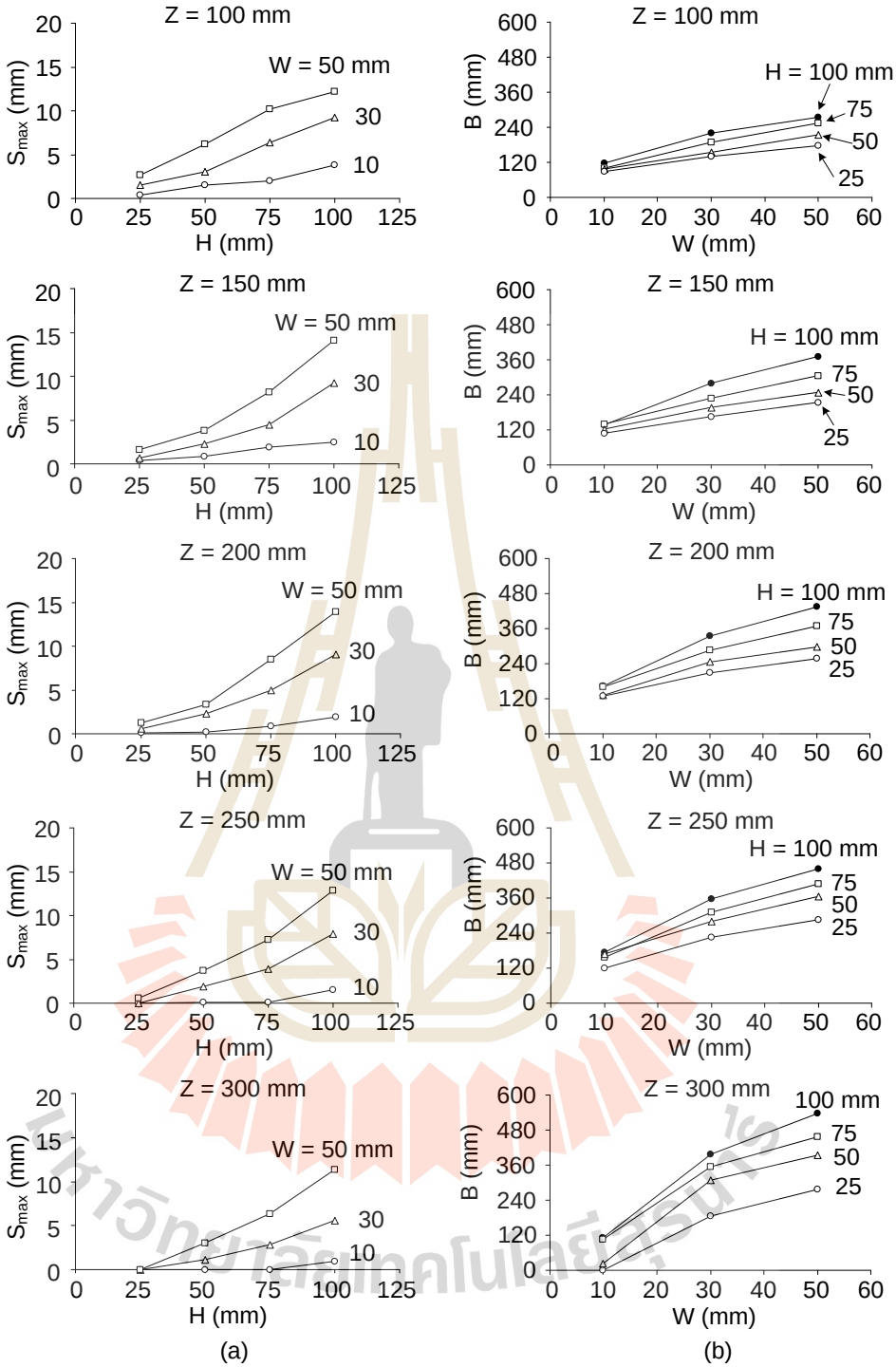

Figure 4.8 (a) S_{max} as a function of H, and (b) B as a function of W for friction angle of 35°.

CHAPTER V

MATHEMATICAL RELATIONSHIPS

5.1 Introduction

This chapter describes a method to estimate the geometry of salt-solutioned cavern from subsidence trough configuration. The results from the physical model and numerical simulation are used to derive from subsidence of mathematical relationships between the surface subsidence component and the cavern configurations and overburden properties. The considered variables are the opening height (H), opening width (W), maximum subsidence (S_{max}), trough width (B), thickness of the overburden or opening depth (Z), and friction angle (ϕ) of overburden material. The empirical equations are developed for the surface subsidence under super-critical conditions.

5.2 Empirical equations

The opening height (H), opening width (W), maximum subsidence (S_{max}), trough width (B) and opening depth (Z) are first equivalented by size of test particle (2 mm), as shown in Figures 5.1 and 5.2. This approach can isolate the particle size effect, and hence allows us to correlate the modeling results with the actual field condition where the particle sizes of the overburden may be larger. Table 5.1 shows the equivalent subsidence components with 2 mm particle size. The equivalent opening height (H_e), opening width (W_e), maximum subsidence (S_e), trough width (B_e), and opening depth (Z_e) can be expressed as:

$$H_e = H/B_s \quad (5.1)$$

$$W_e = W/B_s \quad (5.2)$$

$$S_e = S_{max}/B_s \quad (5.3)$$

$$B_e = B/B_s \quad (5.4)$$

$$Z_e = Z/B_s \quad (5.5)$$

where B_s is particles size of fine sand with nominal size 2mm.

Table 5.1 Equivalent subsidence component.

Z_e	W_e	H_e	S_e	B_e
50	5	50	2.25	60.33
		37.5	1.35	52.52
		25	1.05	50.52
		12.5	0.54	46.92
	15	50	4.94	110.15
		37.5	3.5	97.04
		25	1.8	80.06
		12.5	1.075	71.78
	25	50	6.415	139.32
		37.5	5.4	129.70
		25	3.35	109.31
		12.5	1.61	90.30
75	5	50	1.5975	70.49
		37.5	1.2975	69.55
		25	0.78	62.00
		12.5	0.525	55.21
	15	50	4.9725	140.41
		37.5	2.5725	114.52
		25	1.4475	99.54
		12.5	0.66	84.47
	25	50	7.29	187.03
		37.5	4.4475	153.46
		25	2.1525	125.46
		12.5	1.14	107.83

Table 5.1 Equivalent subsidence component (Cont.).

Z_e	W_e	H_e	S_e	B_e
100	5	50	1.25	82.95
		37.5	0.75	80.62
		25	0.4	67.21
		12.5	0.34	65.19
	15	50	4.8	168.00
		37.5	2.8	144.53
		25	1.4	125.19
		12.5	0.61	106.36
	25	50	7.18	218.33
		37.5	4.5	186.47
		25	1.95	150.04
		12.5	0.91	129.71
125	5	50	1.1	90.00
		37.5	0.4	81.00
		25	0.5375	73.46
		12.5	0.4375	62.50
	15	50	4.25	180.50
		37.5	2.2625	157.00
		25	1.25	142.50
		12.5	0.35	114.50
	25	50	6.75	231.00
		37.5	3.95	207.50
		25	2.125	184.50
		12.5	0.6	145.43

Table 5.1 Equivalent subsidence component (Cont.).

Z_e	W_e	H_e	S_e	B_e
150	5	50	0.75	87.50
		37.5	0.27	64.95
		25	0.18	38.34
		12.5	0	0
	15	50	3	200.45
		37.5	1.755	178.79
		25	0.9	156.84
		12.5	0.03	125.48
	25	50	6.045	269.75
		37.5	3.45	229.98
		25	1.8	198.50
		12.5	0.495	160.38

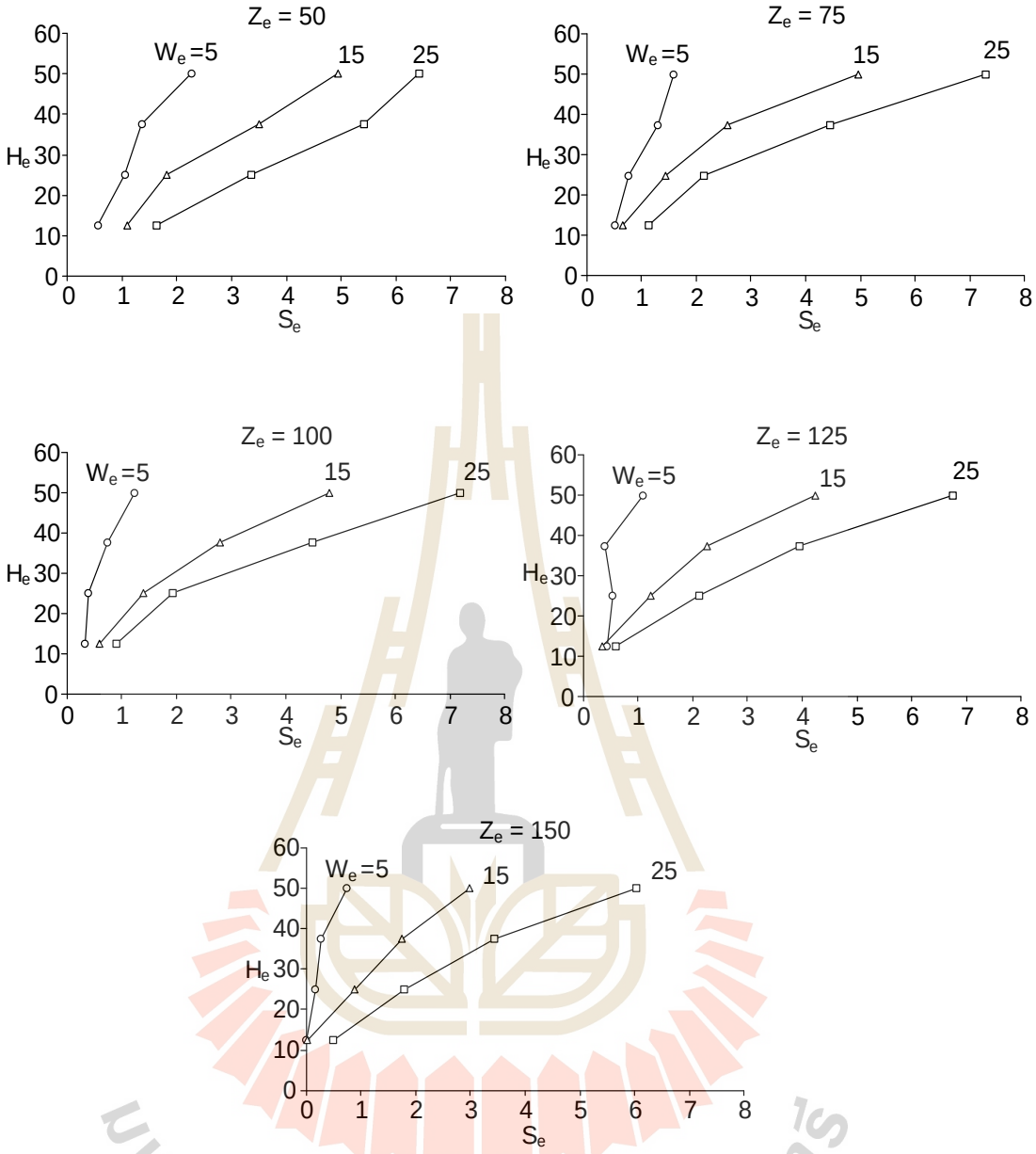

Figure 5.1 Equivalent opening height (H_e) as a function of equivalent maximum subsidence (S_e) for different equivalent depth (Z_e).

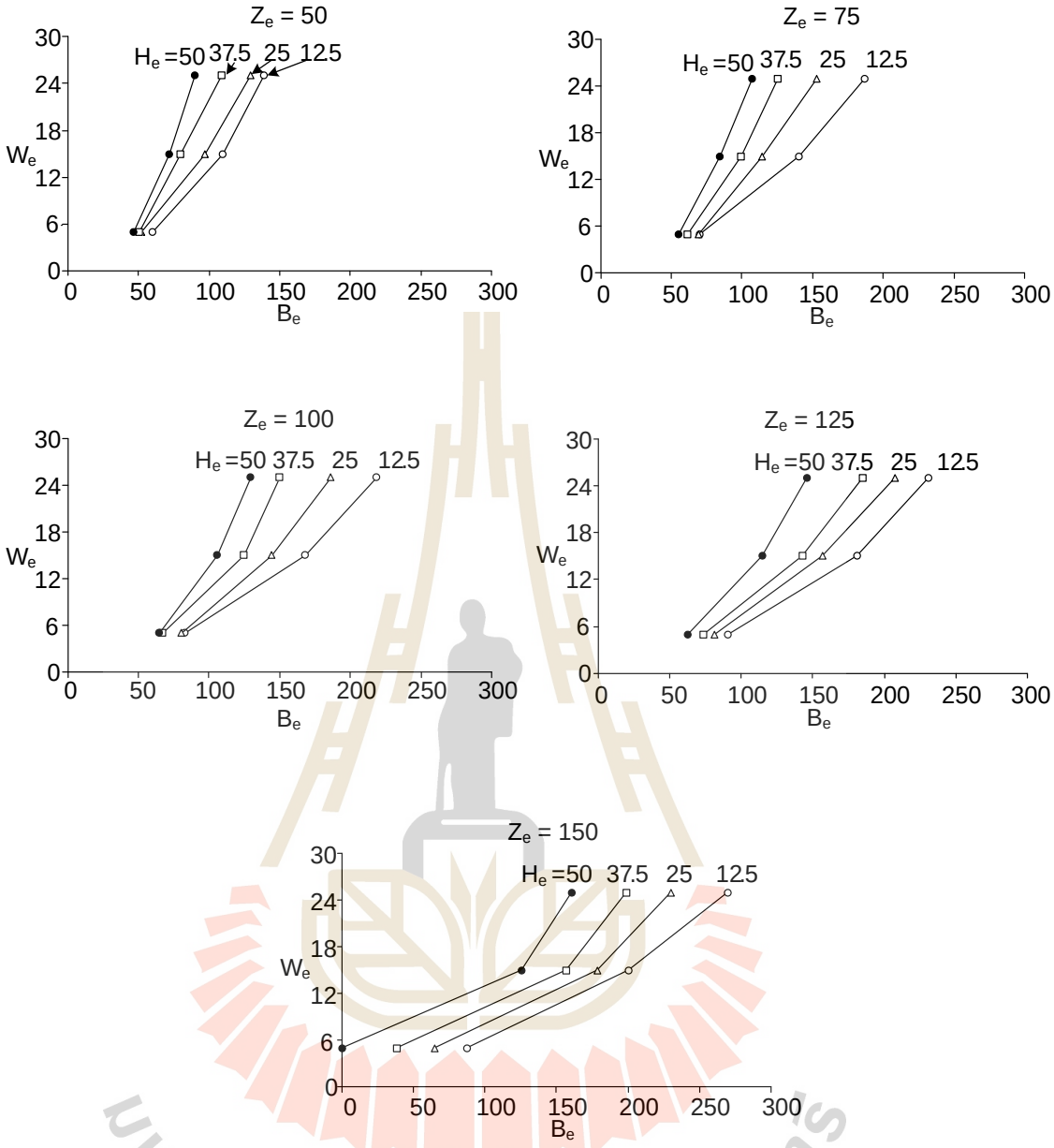

Figure 5.2 Equivalent opening width (W_e) as a function of equivalent trough width (B_e) for different equivalent depth (Z_e).

Figure 5.3 plots the equivalent opening height (H_e) as a function of equivalent subsidence which is normalized by the equivalent opening depth (S_e/Z_e). Empirical equation is proposed to represent the equivalent opening height as a function of normalized subsidence, as follows:

$$H_e = A \cdot S_e/Z_e^B \tag{5.6}$$

where A and B are empirical constants. Based on linear regression analyses of the results from the physical models in Figure 5.3 it is found that the parameter A tends to be constant at 1600. The parameter B can be defined as a function of equivalent trough width (B_e) and equivalent opening depth (Z_e), as follows:

$$B = \alpha \cdot (B_e/Z_e) + \beta \tag{5.7}$$

where α and β are constants which equal to 0.6 and 0.41. They probably depend on the properties of the sand overburden.

Figure 5.4 shows the equivalent opening width (W_e) as a function of equivalent trough width that is normalized by the equivalent opening depth (B_e/Z_e). Similar to the equivalent height in equation (5.6) above, an empirical equation can be proposed to represent the opening width as a function of normalized subsidence obtained from the physical model results, as follows:

$$W_e = [-C \cdot \ln(S_e/Z_e) + D] \cdot B_e/Z_e \tag{5.8}$$

where C and D are empirical constants, and remain constant at 1.66 and 5.85, respectively.

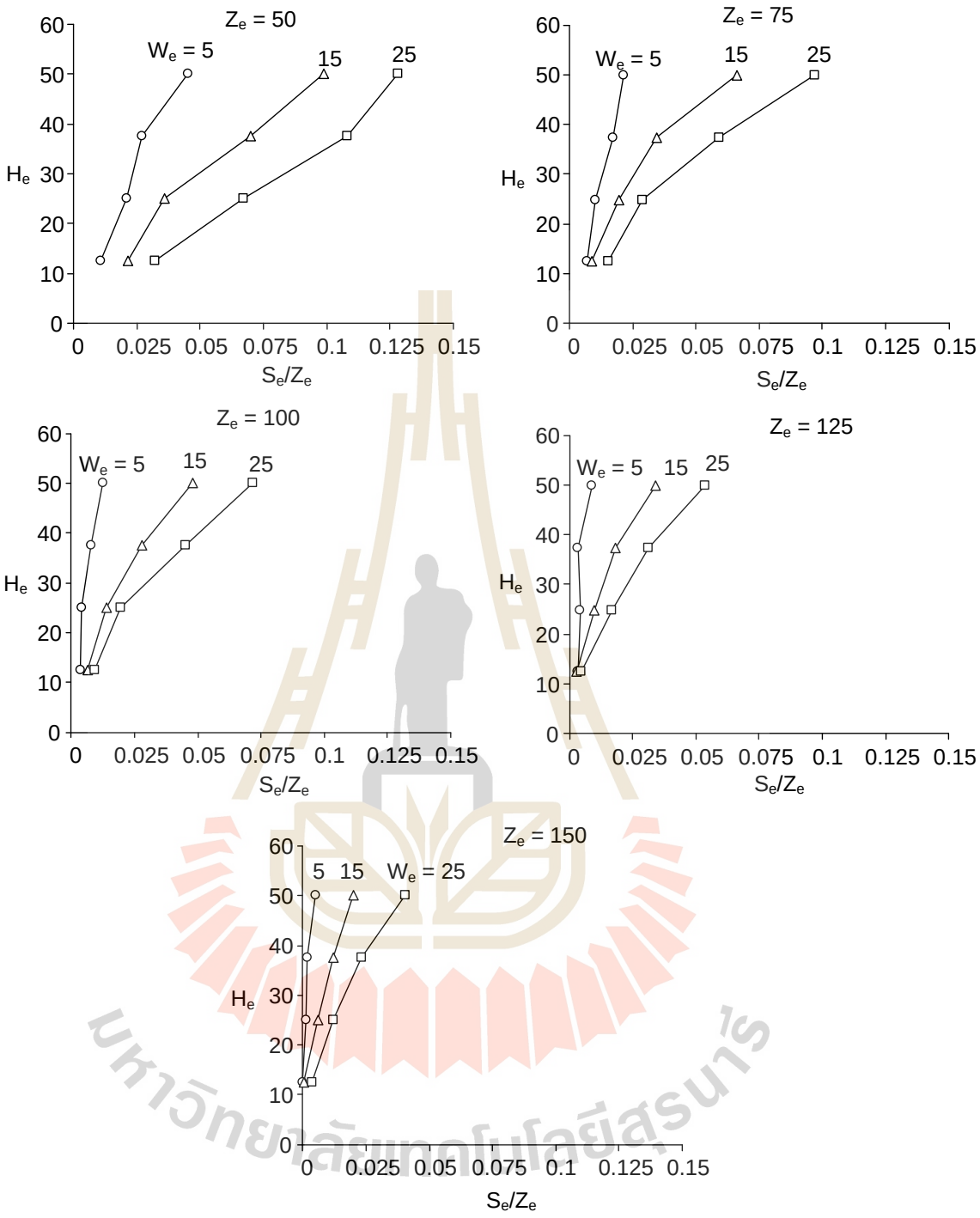

Figure 5.3 Equivalent opening height (H_e) as a function of normalized maximum subsidence (S_e/Z_e).

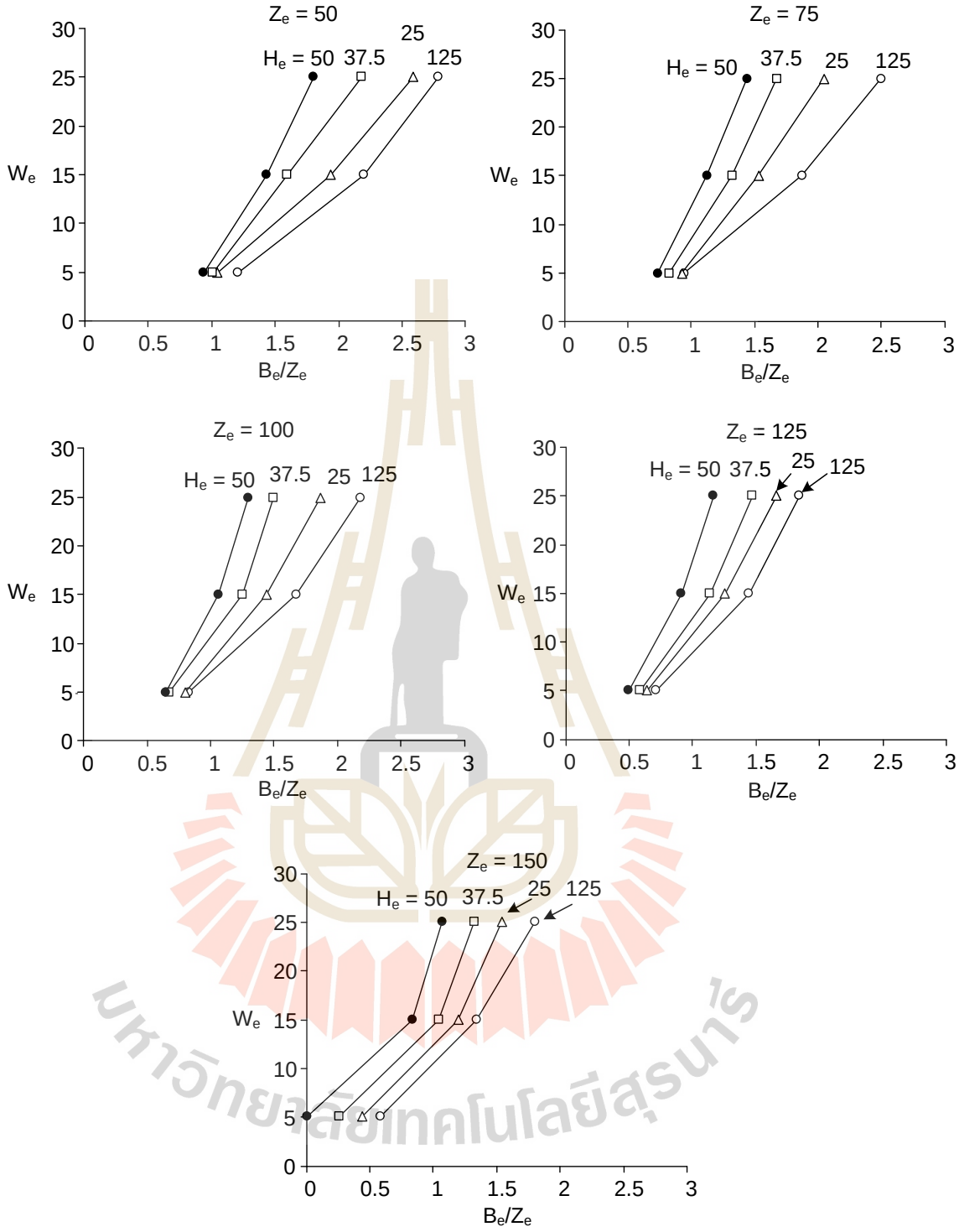

Figure 5.4 Equivalent opening width (W_e) as a function of normalized trough width (B_e/Z_e).

5.3 Overburden Properties Considerations

To find the relationship between the empirical constants in the equations above and the overburden properties, series of numerical simulations are performed using the particle friction angles varying from 20, 25, 30 to 35 degrees. Figure 5.5 compares the numerical model results with the predictions given by equations (5.6) and (5.7). The equivalent opening height (H_e) as a function of normalized maximum subsidence (S_e/Z_e) for various normalized opening widths (B_e/Z_e) obtained from the equations agrees well with the computer simulations. For each width, the opening height increases with the maximum subsidence S_e/Z_e, which can be described by the power equation. Figures 5.6 and 5.7 show the constants α and β from equation (5.7) as a function of friction angles. It is found that the empirical constants α and β depend on the friction angles (ϕ) of the overburden which can be described by a linear equation:

$$\alpha = -0.0236(\phi) + 1.1242 \tag{5.9}$$

$$\beta = 0.0103(\phi) + 0.1732 \tag{5.10}$$

where ϕ used in the computer simulations are 20, 25, 30, and 35 degrees. Figure 5.8 and 5.9 show the equivalent opening height as a function of normalized maximum subsidence for various normalized opening widths at friction angles of 20 and 35 degrees.

The equivalent opening width (W_e) increases with increasing normalized trough width (B_e/Z_e) based on the results of physical models for overburden friction angle of 22.7 degrees, as shown in Figure 5.10. Similar to the equivalent opening width

equations above, the equivalent opening height can be expressed as a function of S_e/Z_e. These parameters are independent of the friction angle of the overburden.

It should be noted that the maximum subsidence and trough width in the equations above are normalized by the equivalent opening depth. The depth of the solutioned cavities are usually known from the depth of the pumping wells used to draw the brine directly above the salt bed.

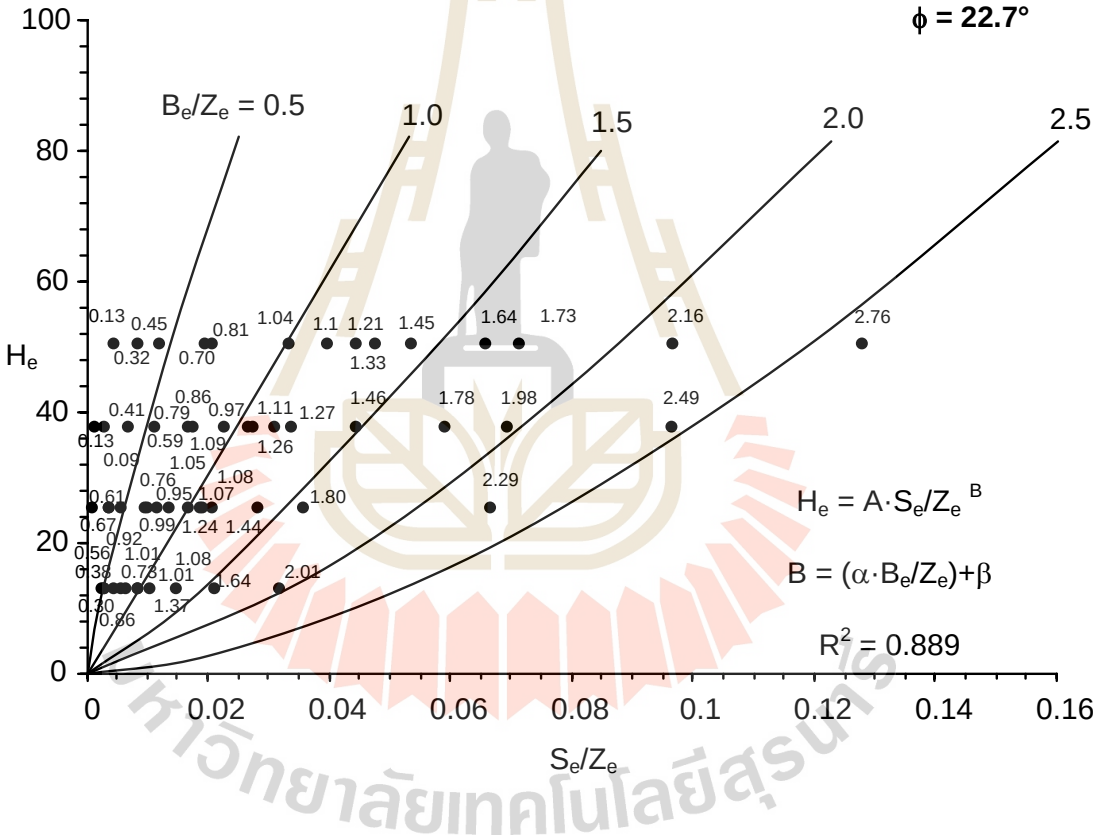

Figure 5.5 Curve fits for equivalent opening height (H_e) compared with results of physical models.

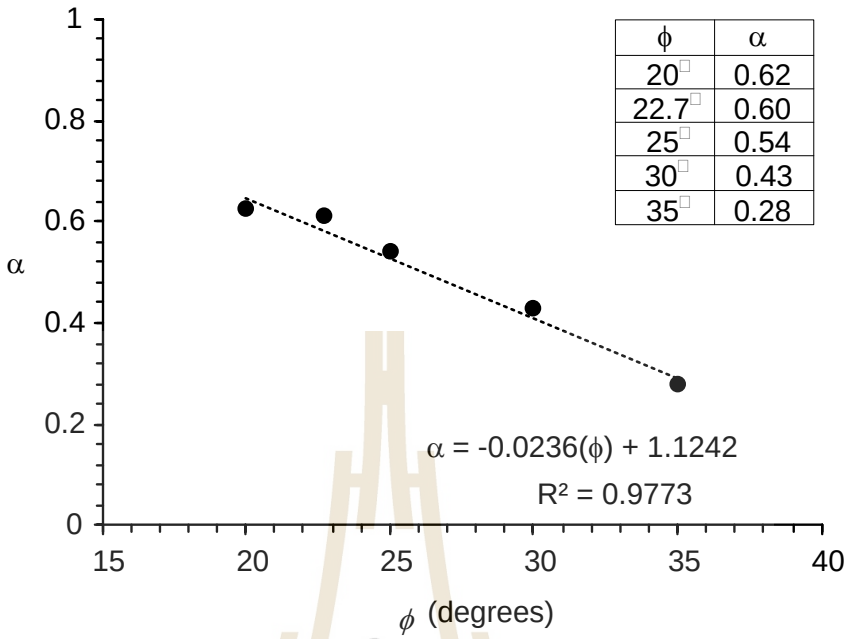

Figure 5.6 Constant α as a function of friction angle (ϕ).

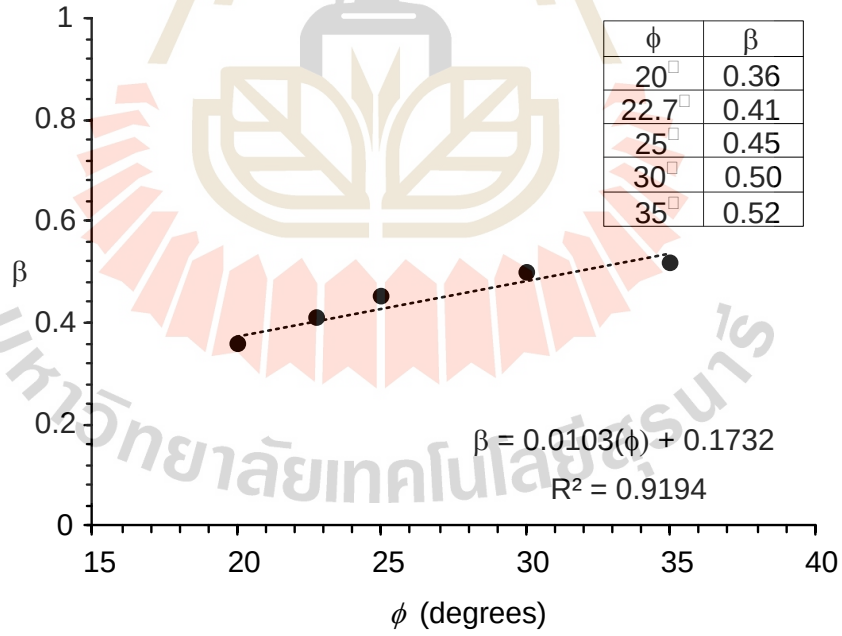

Figure 5.7 Constant β as a function of friction angle (ϕ).

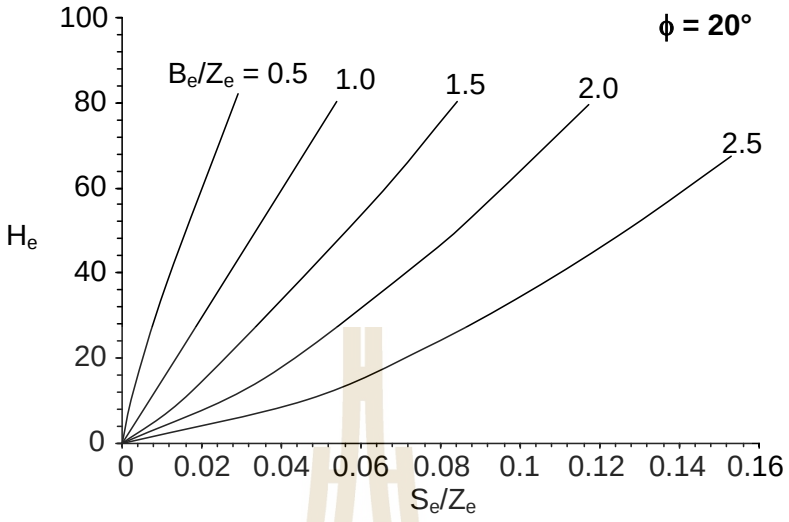

Figure 5.8 Curve fits for equivalent opening height (H_e) compared with the computer simulations of friction angle 20 degrees.

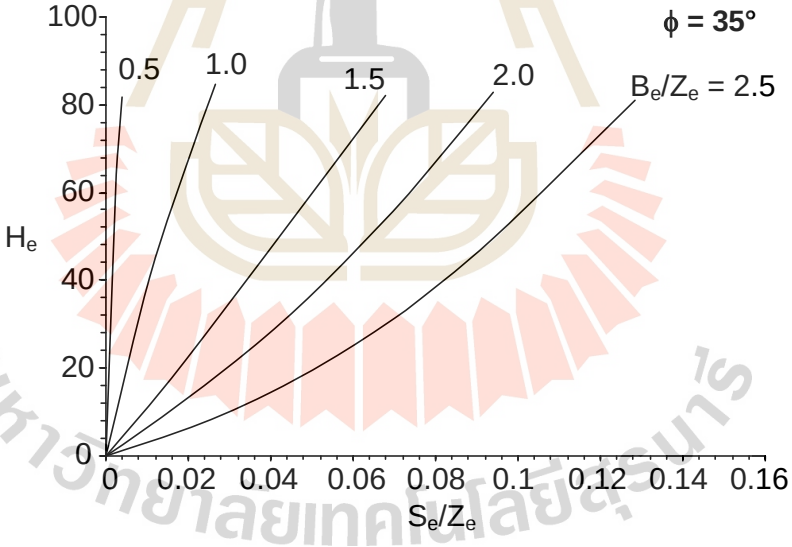

Figure 5.9 Curve fits for H_e compared with the computer simulations of friction angle 35 degrees.

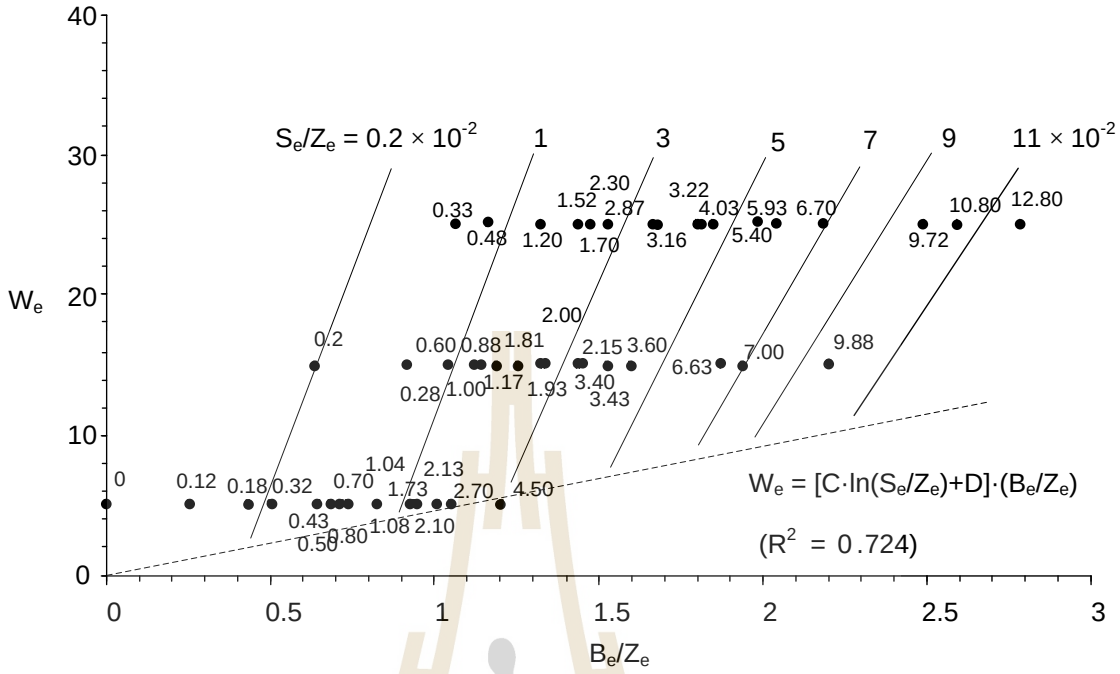

Figure 5.10 Curve fits for equivalent opening height (W_e) compared with the computer simulations (point).

CHAPTER VI

DISCUSSIONS, CONCLUSIONS AND RECOMMENDATIONS FOR FUTURE STUDIES

6.1 Discussions

This section discusses the key issues relevant to the reliability of the physical model and the adequacies of the test results. Comparisons of the results and findings from this study with those obtained from observations by other researchers have been made.

The results from PFC^{2D} simulations agree well with the measurements from the physical model, suggesting that the test results are sufficiently reliable. Physical models are tested under super-critical condition, the overburden material is cohesionless (c = 0) due to the collapse of the cavern roof and overburden, which is dictated by the cavern height. If the cavern height is greater than the critical roof deformation, failure of the cavern roof can occur under the super-critical condition (Fuenkajorn and Archeeploha, 2009). The test results obtained here agree reasonably well with those of Thongprapha et al. (2015) who study the surface subsidence above underground opening using gravel.

Physical models have been performed to simulate surface subsidence of overburden in 3-dimension. The highest opening depth (Z) which is 300 mm seems to limit the higher ends of opening depths for all test. This thickness of overburden

material is suitable for the scaled-down platform or trap door apparatus. The higher opening depth produce lower subsidence which cannot be measured in the available device.

The physical model results clearly indicate that the S_{max}, γ, and B are controlled by the geometrical characteristics of underground opening and overburden thickness. This finding supports previous study that the extend of the surface subsidence affected area is defined by trough width (B) and angle of draw (γ), which is controlled predominantly by geological conditions of the overburden strata and the geometry of underground opening. This agrees with experimental observations by Park et al. (2004), Fuenkajorn and Archeeploha (2009), Thongprapha et al. (2015) and Saoanunt and Fuenkajorn (2015) who study surface subsidence under super critical condition by using analytical method, physical models, and discrete element analyses.

The measurement results from physical models and numerical simulations indicate that the increase of the S_{max} closely relates to the increase of H, while the increase of B is related to the increase of W. The S_{max} values tend to be independent of the Z while W is more sensitive to the Z. This supports the postulation given by Singh (1992) that under super-critical subsidence condition the maximum subsidence tends to be constant, while the trough width tends to increase with the opening width.

An assessment of the effect of the friction angles of overburden material have been performed by using computer simulation. The varied friction angles from 20, 25, 30, to 35 degrees have been made under varied H, W and Z. The results obtained from this approach indicate that the friction angle affects the surface subsidence. The S_{max}, B and γ decrease with increasing friction angles. This finding, while preliminary,

suggest that the friction angle can affect the surface subsidence even under the same geometry of underground opening.

From equation (5.6), parameter B is probably depends on the friction angle of the overburden, as shown in equations (5.8 and 5.9). This finding can be concluded that the friction angle is governed by the opening height but not the opening width.

The proposed equations above can be used individually to estimate the opening height (H) and opening width (W). The equations are obtained from combining the physical models and numerical simulations (S_{max}, and B) to determine the mathematical relationships. All results are equivalented to isolate the effect of particle size (see equations 5.1-5.5) and normalized opening depths. The equivalent opening height (H_e) by the function can be separated by power equation, while the equivalent opening width (W_e) by linear equation. The H_e is largely governed by the maximum subsidence (S_{max}), while W_e is controlled by trough width (B), as suggested by the physical model results.

6.2 Conclusions

All objectives and requirements of this study have been met. The results of the physical models, numerical simulations and empirical equations can be concluded as follows:

The close agreement between the physical model measurements and numerical simulations suggests that the procedure and results of the physical modelling are accurate and reliable.

Both approaches indicate that the increase of the maximum subsidence closely relates to the increase of opening height, while the increase of trough widths is related to the increase of opening width. The maximum subsidence values tend to be

independent of the opening depths or overburden thickness. The trough width however is more sensitive to the overburden thickness.

The results obtained from the numerical simulations (PFC^{2D}) of the varied friction angles of overburden material indicate that the surface subsidence magnitudes decrease with increasing the friction angle.

The proposed mathematical equations may be used as a predictive tool to estimate the cavern height and width of Maha Sarakham formation based on the subsidence trough size and shape and the friction angle of the overburden materials in super-critical condition. Subsequently, remedial measure may be implemented to minimize the impact from the cavern development before severe subsidence or sinkhole occurs.

6.3 Recommendations for future studies

The uncertainties and adequacies of the study and results discussed above lead to the recommendations for future studies.

The effect of topography and inclination of contact surface should also be studied.

The effect of vertical and horizontal stresses on subsidence trough should be studied for each overburden thickness.

The effect of the groundwater should be assessed by physical model and numerical simulations.

The overburden material with different friction angle should be tested confirm the empirical equations propose here.

Different particles sizes should be used in the physical model to study the behavior of surface subsidence under various equivalent variables.

Comparison of the predictions using the proposed equations with the actual in-situ conditions are derivable to enhance the applicability of the findings obtained here.

REFERENCES

Adachi, T., Kimura, M. and Kishida, K. (2003). Experimental study on the distribution of earth pressure and surface settlement through three-dimensional trapdoor tests. **Tunnelling and Underground Space Technology**. 18: 171-183.

Alejano, L R., Ramirez-Oyanguren, P. and Taboada, J. (1999). FDM predictive methodology for subsidence due to flat and inclined coal seam mining. **International Journal of Rock Mechanics and Mining Sciences**. 36: 475-491.

Aracheeploha, S., Horkaew, P., and Fuenkajorn, K. (2009). Prediction of cavern configurations from subsidence data. In **Proceedings of the Second Thailand Symposium on Rock Mechanics** (pp. 116-176). Chonburi: Suranaree University of Technology.

Asadi, A., Shahriar, K., Goshtasbi, K., and Najm, K. (2005). Development of new mathematical model for prediction of surface subsidence due to inclined coal-seam mining. **Journal of the Southern African Institute of Mining and Metallurgy.** 105(11): 15-20.

ASTM Standard D2487–06. (2006). **Standard Practice for Classification of Soils for Engineering Purposes (Unified Soil Classification System).** Annual Book of ASTM Standards, American Society for Testing and Materials, West Conshohocken, PA.

ASTM Standard D422–63. (2007). **Standard Test Method for Particle-Size Analysis of Soils.** Annual Book of ASTM Standards, American Society for

Testing and Materials, West Conshohocken, PA.

ASTM Standard D5607–08. (2008). **Standard Test Method for Performing Laboratory Direct Shear Strength Tests of Rock Specimens Under Constant Normal Force.** Annual Book of ASTM Standards, American Society for Testing and Materials, West Conshohocken, PA.

Atkinson, J. H. and Potts, D. (1977). Subsidence above Shallow Tunnels in Soft Ground. **Journal of the Geotechnical Engineering Division.** 103(4): 307-325.

Attewell, P. B. (1977). Ground movements caused by tunnelling in soil. Cardiff J.D. Geddes (Ed.), In **first Conference on Large Ground Movements and Structures.** Pentech Press, London pp. 812–948.

Bahuguna, P. P., Srivastava, A. M. C., and Saxena N. C. (1991). A critical review of mine subsidence prediction methods. **Mining Science and Technology**. 15: 369-382.

Barton, N. R. (1974). A review of the shear strength of filled discontinuities in rock. **Norwegian Geotechnology Institute of Oslo**. pp. 105.

Bobet, A. (2001). Analytical Solutions for Shallow Tunnels in Saturated Ground. **Journal of Engineering Mechanics.** 127(12): 1258-1266.

Caudron, M., Emeriault, F., Kastner, R., and Al Heib, M. (2006). Sinkhole and soil-structure interaction: Development of an experimental model. In **Proceedings of International Conference on Physical Modeling in Geotechnics.** Hong-Kong. (pp. 1261-1267).

Chi, S. Y., Chern, J. C., and Lin, C. C. (2001). Optimized back-analysis for tunnelinginduced ground movement using equivalent ground loss model. **Tunnelling and Underground Space Technology**. 16(3): 159-165.

Chou, W. I., and Bobet, A. (2002). Predictions of ground deformations in shallow tunnels in clay. **Tunnelling and Underground Space Technology.** 17(1): 3-19.

Clough, G. W. and Schmidt, B. (1981). Design and performance of excavations and tunnels in soft clay. **Soft Clay Engineering** (Chapter 8).

Crosby, K. (2007). Integration of rock mechanics and geology when designing the Udon South sylvinite mine. **Proceedings of the First Thailand Symposium on Rock Mechanics,** Nakhon Ratchasima: Suranaree University of Technology. pp. 3-22. Thailand.

Cundall, P. A. and Strack, O. D. L. (1979). A discrete numerical model for granular assemblies. **Geotechnique.** 29(1): 107-116.

Fuenkajorn, K. (2002). Design guideline for salt solution mining in Thailand. **Research and Development Journal of the Engineering Institute of Thailand.** Vol. 13(1): 1-8.

Fuenkajorn, K. and Aracheeploha, S. (2011). Prediction of cavern configurations from subsidence data. **Engineering Geology.** 110: 21-29.

Galli, G., Grimaldi, A. and Leonardi, A. (2004). Threedimensional modeling of tunnel excavation and lining. **Computers and Geotechnics.** 31: 171-183.

Ghabraie B., Ren G., Ghabraie, K., Xie Y. and Smith, J. (2014). Physical modeling ofsubsidence from sequential extraction of partially overlapping longwall panels and study of substrata movement characteristics. **International Journal of Coal Geology.** 80: 219-230.

Gonzales, C., and Sagesta, C. (2001). Patterns of soil deformation around tunnels. Application to the extension of the Madrid Metro. **Computers and**

Geotechnics. 28: 445-468.

Grøneng, G., Nilsen, B., and Sandven, R. (2009). Shear strength estimation for Åknes sliding area in western Norway. **International Journal of Rock Mechanics and Mining Sciences.** 46 (3), pp. 479-488.

Helm, P. R., Davie, C.T. and Glendinning, S. (2013). Numerical modelling of shallow abandoned mine working subsidence affecting transport infrastructure. **Engineering Geology**. 154: 6-19.

Hawkes, T. P. (2010). A Simple Aprroach to Subsidence Prediction Above Longwall Mines. **Brigham Toung University**.

Itasca, 2008a, **PFC^{2D}–Particle Flow Code in 2 Dimensions, Version 4.0**, User Manual, Itasca Consulting Group Inc., Minnespolis, MN, USA.

Itasca, 2008b, **User manual for PFC3D–Particle Flow Code in 3 Dimensions, Version 4.0**, Itasca Consulting Group Inc., Minnespolis, MN, USA.

Jenkunawat, P. (2005). Results of drilling to study occurrence of salt cavities and surface subsidence Ban Non Sabaeng and Ban Nong Kwang, Amphoe Ban Muang, Sakon Nakhon. **International Conference on Geology, Geotechnical and Mineral Resources of Indochina (GEOINDO 2005)**, Khon Kaen: Khon Kaen University. pp. 259-267.

Jenkunawat, P. (2007). Results of drilling to study occurrence of salt cavities and surface subsidence Ban Non Sabaeng and Ban Nong Kwang, Sakon Nakhon. **Proceedings of the First Thailand Symposium on Rock Mechanics,** Nakhon Ratchasima: Suranaree University of Technology. pp. 257-274.

Ju, M., Li, X., Yao, Q., Liu, S., and Wang, X. (2007). Effect of sand grain size on simulated mining-induced overburden failure in physical model tests.

Engineering geology. 226: 93-106.

Li, X. Q. and Zhu, C. C. (2007). Numerical Analysis on the Ground Settlement Induced by Shield Tunnel Construction. **Journal of Highway and Transportation Research and Development (English Edition).** 2(2): 73-79.

Li, Z. and Wang, J. (2011). Accident investigation of mine subsidence with application of particle flow code. **Procedia Engineering.** 26: 1698–1704.

Lisjak A. and Grasselli G., (2004). A review of discrete modelling techniques for fracturing process in discontinuous rock masses. **Journal of Rock Mechanics and Geotechnical Engineering.** 6: 301-314.

Liu, Y., Zhou, F., Liu, L., Liu, C. and Hu, S. (2011). An experimental and numerical investigation on the deformation of overlying coal seams above double-seam extraction for controlling coal mine methane emissions. **International Journal of Coal Geology.** 87: 139 – 149.

Loganathan, N. and Poulos, H. (1998). Analytical prediction for tunneling-induced ground movements in clays. **Journal of Geotechnical and Geoenvironmental Engineering.** 124(9): 846-856.

Mair, R. J., Taylor, R. N. and Bracegirdle, A. (1993). Subsurface settlement profiles above tunnels in clays. **Geotechnique.** 43(2): 315–320.

Meguid, M.A., Saada, O., Nunes, M.A. and Mattar, J. (2008). Physical modeling of tunnels in soft ground: A review. **Tunnelling and Underground Space Technology**. 23: 185-198.

Mcnearny, R. L. and Barker, K. A. (1998). Numerical modeling of large-scale block cave physical models using PFC2D. **Mining Engineering.** 50(2): 72-75.

National Coal Board, **Subsidence Engineer's Handbook Mining Dep.**, National Coal Board, London, (1975) 111 pp.

O'Reilly, M. P. and New, B. M. (1982). Settlements above tunnels in the United Kingdom - their magnitude and prediction. **Tunnelling 82, The Institution of Mining and Metallurgy** (pp. 55–64). London.

Parise M and Lollino P., (2011). A preliminary analysis of failure mechanisms in karst and man-made underground caves in Southern Italy. **Geomorphology.** pp.132–143.

Park, D. and Li, J. (2004). Subsidence Simulation Using Laser Optical Triangulation Distance Measurement Devices. In **Gulf Rocks 2004, the Sixth North America Rock Mechanics Symposium (NARMS)** (pp. 6). Houston, Texas.

Peck, R. B. (1969). Deep excavations and tunneling in soft ground. In **Proceedings of the Seventh international conference on soil mechanics and foundation engineering, State of the art.** Sociedad Mexicana de Mecánica de Suelos (pp. 225–290).

Peng, S. S. (1992). Surface subsidence engineering. **New York: Society of Mining Engineers**.

Sagaseta, C. (1987). Analysis of undraind soil deformation due to ground loss. **Géotechnique**. 37(3): 301-320.

Saoanunt, N. and Fuenkajorn, K. (2015). Physical model simulations of super-critical subsidence as affected by mining sequence and excavation rate. In **ninth South East Asia Technical University Consortium (SEATUC) Symposium,** Suranaree University of Technology. pp. 22-25. Thailand.

Sartkeaw, S. and Fuenkajorn, K. (2016). Verifications of empirical method and numerical simulation using physical model for subsidence prediction of maha sarakham formation. **Research and Development Journal of the Engineering Institute of Thailand under H.M. the King's Patronage.** Vol. 27(3) :17-24**.**

Satarugsa, P., Youngmee, W., and Meesawat, S. (2005). New regional boundary of MahaSarakham Formation in the Northeastern Thailand: results from 2D seismic mapping. In: Wannakao, L., Youngmee, W., Sirsuk, K., and Lertsirivorakul, R. (eds), In **Proceedings on International Conference on Geology, Geotechnology and Mineral Resources of Indochina (GEOINDO 2005),** Khon Kaen: Khon Kaen University. pp. 212-220. Thailand.

Satarugsa, P., Youngmee, W., and Meesawat, S., (2011). The Lessons Learnt from Geophysical Investigation of Sinkholes in Rock Salt in Thailand. **International Conference on Geology, Geotechnology and Mineral Resources of Indochina (GEOINDO 2011).** Khon Kaen: Khon Kaen University. pp. 445-455. Thailand.

Singh, M. M. (1992). **Mine subsidence**. In: SME Mining Engineering Handbook. Hartman, H.L. (ed). Society for Mining Metallurgy and Exploration, Inc., Littleton, Colorado, pp. 938-971.

Suwanich, P. (1986). **Potash and Rock Salt in Thailand: Nonmetallic Minerals Bulletin No.2,** Economic Geology Division, Department of Mineral Resources, Bangkok, Thailand.

Terzaghi, K. (1936). Stress distribution in dry and in saturated sand above a yielding trap-door. In **Proceeding of the International Conference on Soil Mechanics** (pp. 307-311). Cambridge.

Thongprapha, T., Fuenkajorn, K., and Daemen, J. J. K. (2015). Study of surface subsidence above an underground opening using a trap door apparatus. **Tunnelling and Underground Space Technology.** 46: 94–103.

Unlu, T., Akcin, H., and Yilmaz, O. (2013). An integrated approach for the prediction of subsidence for coal mining basins. **Engineering Geology**: 166, 186–203.

Vattanasak, H. (2006). Salt reserve estimation for solution mining in the Korat basin, M.Eng Thesis, Nakhon Ratchasima: Suranaree University of Technology.

Verruijt, A., and Booker, J. (1996). Surface settlements due to deformation of a tunnel in an elastic half plane. **Géotechnique.** 46(4): 753-756.

Wang, J. G., Leung, C. F., and Chow Y. K. (2003). Numerical solutions for flow in porous media. **International Journal for Numerical and Analytical Methods in Geomechanics.** 27(7): 565-583

Wannakao, L. and Walsri, C. (2007). Subsidence models in salt production area. **Proceedings of the First Thailand Symposium on Rock Mechanics,** Nakhon Ratchasima: Suranaree University of Technology. pp. 311-321.

Wannakao, L., Munjai, D., and Janyakorn, S. (2005). Geotechnical investigation of surface subsidence at Ban Non Sabaeng salt production area, Sakon Nakhon, Thailand. **International Conference on Geology, Geotechnical and Mineral Resources of Indochina (GEOINDO 2005).** Khon Kaen: Khon Kaen University. p. 282.

Whittaker, B. N. and Reddish, D. J. (1989). Subsidence Occurrence, Prediction and Control. Amsterdam: **Elsevier Science Publishers**. 56.

BIOGRAPHY

Miss Naruemol Saoanunt was born in January 12, 1991 in Buriram province, Thailand. She received her Bachelor's Degree in Engineering (Geotechnology) from Suranaree University of Technology in 2014 and received her Master's Degree in Engineering (Geotechnology) from Suranaree University of Technology in 2016. For her post-graduate, she continued to study with a Doctor of Philosophy Program in Civil, Transportation and Geo-resources Engineering, Institute of Engineering, Suranaree university of Technology, she was a part time worker in position of research assistant at the Geomechanics Research Unit, Institute of Engineering, Suranaree University of Technology. She published technical paper related to rock mechanics, titled Estimation of salt-solutioned cavern geometry from subsidence trough configurations under super-critical condition in the Research and Development Journal of the Engineering Institute of Thailand (EIT) under H.M. the King's Patronage.